Multivariate Varying-coefficient Models via Tensor Decomposition

Fengyu Zhang, Ya Zhou, Kejun He, and Raymond K. W. Wong

Renmin University of China, Chinese Academy of Medical Sciences and Peking Union Medical College,

Renmin University of China, and Texas A&M University

Abstract: Multivariate varying-coefficient models are popular statistical tools for analyzing the relationship between multiple responses and covariates. Nevertheless, estimating large numbers of coefficient functions is challenging, especially with limited samples. In this work, we propose a reduced-dimension model based on the Tucker decomposition that unifies several existing models. In addition, we use sparse predictor effects, in the sense that only a few predictors are related to the responses, to achieve an interpretable model and sufficiently reduce the number of unknown functions to be estimated. These dimension-reduction and sparsity considerations are integrated into a penalized least squares problem on the constraint domain of third-order tensors. To compute the proposed estimator, we propose a block updating algorithm based on the alternating direction method of multipliers and manifold optimization. We also establish the oracle inequality for the prediction risk of the proposed estimator. A real data set from the Framingham Heart Study is used to demonstrate the good predictive performance of the proposed method.

Key words and phrases: Tucker low rank; group lasso; dimensionality reduction; polynomial splines; sparsity.

The first two authors contributed equally to this work. Kejun He (Email: kejunhe@ruc.edu.cn) is the corresponding author.

1. Introduction

Varying-coefficient models (VCMs, Hastie and Tibshirani, 1993) are popular structured regression models that have reasonably flexible nonparametric components and can be estimated well with a moderate amount of data (Ruppert et al., 2003). In VCMs, the regression coefficients of the predictors vary with an observable exposure variable. VCMs have been studied extensively in literature and are widely used in practice; see, for example, Hoover et al. (1998), Huang et al. (2002), Park et al. (2015), and the references therein. For settings with a large number of predictors (possibly larger than the sample size), Wang et al. (2008) use basis function expansions and the smoothly clipped absolute deviation (SCAD) penalty to address the problem of variable selection. Wei et al. (2011) and Lian (2012) apply an adaptive group least absolute shrinkage and selection operator (lasso) and spline function approximations to simultaneously identify the relevant predictors and estimate the varying-coefficient functions of those that have been selected. The latter works also obtain the rate of convergence and variable-selection consistency for their estimators under suitable conditions. Xue and Qu (2012) use a truncated ℓ_1-penalty (TLP) to select variables, and obtain the oracle properties for their varying-coefficient estimator. To enhance the computational scalability, feature screening techniques for the VCM are considered in Fan et al. (2014) and Liu et al. (2014), who propose to rank the marginal nonparametric contributions of each predictor, given the exposure variable, and investigate sure independent screening properties.

In many applications, multiple responses are jointly observed with the predictors and the exposure variable. For instance, the Framingham Heart Study (Dawber et al., 1951) collected multiple phenotype variables from patients to identify common factors related to cardiovascu-

lar diseases. Obviously, one can simply model each response variable separately using VCMs. Together, these models are viewed as a regression model for the multivariate response, called an unstructured multivariate varying-coefficient model (MVCM). One challenge associated with such models is the significant number of coefficient functions required to be estimated. More specifically, we need to estimate pq functions if there are p covariates and q responses. To circumvent this problem, one may use structures among these pq functions. He et al. (2018) propose a principal-component-based approach in which they assume the coefficient functions can all be approximated by linear combinations of a much smaller number of unknown functions. However, they do not explore the correlations between the responses, and their method cannot handle the settings with a large number of responses. Lian and Ma (2013) assume a low-rank structure in the conditional means of the responses of the samples. However, their model does not consider the correlations between the predictors and/or the varying coefficients. Furthermore, they do not propose an efficient algorithm to solve their penalized least squares problem.

In this work, we propose a novel method using dimension-reduction tools of tensors (Kolda and Bader, 2009) to handle an MVCM in a high-dimensional setting. In particular, we show that dimension reductions in the predictors, the space of the coefficient functions, and the responses correspond to the low rankness in the first, second, and third modes, respectively, of a third-order tensor. Thus, we propose using the Tucker decomposition (Tucker, 1966) to integrate these three dimension reductions into a simple notion of low multilinear rank. The models of He et al. (2018) and Lian and Ma (2013) can be viewed as special cases of our proposed model. In addition, sparse predictor effects, in the sense that only a few predictors are related to the responses, is often a reasonable assumption in high-dimensional settings. The aforementioned dimension-

reduction and sparsity considerations can be incorporated into the estimation procedure by using a penalized least squares problem on the constraint domain of third-order tensors. To compute the proposed estimator, we design a block updating algorithm based on the alternating direction method of multipliers (ADMM, Boyd et al., 2011) and manifold optimization (Edelman et al., 1998; Absil et al., 2009). We also establish the oracle inequality for the prediction risk of the proposed estimator.

The rest of the paper is organized as follows. In Section 2, we introduce the proposed reduced MVCM using the Tucker decomposition. The estimation method and computational details are presented in Sections 3 and 4, respectively. We establish the oracle inequality for the prediction risk of the proposed estimator in Section 5. We use both a simulation study and a real-data application in Section 6 to illustrate the practical performance of the proposed method. The main contributions of this paper are summarized in Section 7 with some concluding remarks. Technical details are provided in the online Supplementary Material.

2. Model

Let $\boldsymbol{y} = (y_1, \ldots, y_q)^{\mathsf{T}}$, $\boldsymbol{x} = (x_1, \ldots, x_p)^{\mathsf{T}}$, and t be the q-dimensional vector of responses, the p-dimensional vector of predictors, and the exposure variable with compact domain $\mathcal{T}$, respectively. Without loss of generality, we assume $\mathcal{T} = [0, 1]$. Each response is posited to follow a univariate-response VCM, that is,

$$y_l = \sum_{j=1}^{p} f_{jl}(t) x_j + \epsilon_l, \quad l = 1, \ldots, q, \tag{2.1}$$

where $\{f_{jl}(t)\}$ are the coefficient functions and $\{\epsilon_l\}$ are the noise variables, with mean zero and variance σ_l^2. These noise variables are independent of $(\boldsymbol{x}, t)$. By setting $x_1 = 1$, the model can

accommodate an intercept function. In vector-matrix notation, (2.1) can be written as

$$\boldsymbol{y} = \boldsymbol{F}(t)^{\intercal}\boldsymbol{x} + \boldsymbol{\epsilon}, \tag{2.2}$$

where $\boldsymbol{F}(t) = (f_{jl}(t))_{p \times q}$ and $\boldsymbol{\epsilon} = (\epsilon_1, \ldots, \epsilon_q)^{\intercal}$. We call (2.2) the full model of MVCM, in which pq varying-coefficient functions need to be estimated nonparametrically.

When pq is relatively large, there are huge numbers of nonparametric functions, which are difficult to estimate accurately with a small or moderate amount of data. To cope with this challenge, Lian and Ma (2013) assume a rank-R_3 structure on the matrix of coefficient functions, with $R_3 < q$, aiming to reduce the model complexity among the responses. Specifically, Lian and Ma (2013) proposed reducing the full MVCM (2.2) to

$$\boldsymbol{y} = \boldsymbol{C}\widetilde{\boldsymbol{F}}(t)^{\intercal}\boldsymbol{x} + \boldsymbol{\epsilon}, \tag{2.3}$$

where $\boldsymbol{C} \in \mathbb{R}^{q \times R_3}$, with $\boldsymbol{C}^{\intercal}\boldsymbol{C} = \boldsymbol{I}_{R_3}$, and $\widetilde{\boldsymbol{F}}(t)$ is a matrix of $p \times R_3$ unknown functions. Model (2.3) implies that the means of the responses conditional on the predictors and the exposure variable are R_3 linearly dependent among the samples. Compared with (2.2), the number of parameters is reduced to pR_3 functions, together with a $q \times R_3$ coefficient matrix. He et al. (2018) propose a functional principal-component-based approach that assumes all pq coefficient functions can be well approximated by a small number of R_2 unknown data-driven principal functions $\boldsymbol{\beta}(t) = (\beta_1(t), \ldots, \beta_{R_2}(t))^{\intercal}$. More precisely, they assume that the vectorized $\boldsymbol{F}(t)$ can be represented by $\mathrm{vec}\{\boldsymbol{F}(t)\} = \boldsymbol{D}\boldsymbol{\beta}(t)$, with a coefficient matrix $\boldsymbol{D} \in \mathbb{R}^{pq \times R_2}$. Then, the conditional mean of the responses in the full MVCM (2.2) reduces to

$$\mathbb{E}(\boldsymbol{y}|\boldsymbol{x}, t) = \mathrm{vec}\{\boldsymbol{x}^{\intercal}\boldsymbol{F}(t)\} = (\boldsymbol{I}_q \otimes \boldsymbol{x}^{\intercal})\mathrm{vec}\{\boldsymbol{F}(t)\} = (\boldsymbol{I}_q \otimes \boldsymbol{x}^{\intercal})\boldsymbol{D}\boldsymbol{\beta}(t). \tag{2.4}$$

For model identifiability, the principal functions $\boldsymbol{\beta}(t)$ are required to be orthonormal, that is,

$$\int_{\mathcal{T}} \boldsymbol{\beta}(t)\boldsymbol{\beta}(t)^{\mathsf{T}} \, \mathrm{d}t = \boldsymbol{I}_{R_2}.$$

Thus, one only needs to estimate R_2 principal functions and a $p \times R_2 \times q$ coefficient tensor for a reduced MVCM in (2.4). In the univariate-response VCM, that is, $q = 1$, Jiang et al. (2013) propose another principal component VCM. Specifically, treating the lth response in (2.1) as a single response, the model of Jiang et al. (2013) is equivalent to

$$y_l = \boldsymbol{f}_l(t)^{\mathsf{T}} \boldsymbol{A}^{\mathsf{T}} \boldsymbol{x}^{\mathsf{T}} + \epsilon_l, \tag{2.5}$$

where $\boldsymbol{f}_l(t)$ is a vector of R_1 unknown functions, and $\boldsymbol{A} \in \mathbb{R}^{p \times R_1}$ is the principal loading matrix. Overall, Models (2.3), (2.4), and (2.5) encompass dimension reductions within the responses, the coefficient functions, and the predictors, respectively.

However, it is difficult to compare the above models because they employ different methods for dimension reduction. In this work, we observe that these models can be unified into a general model that allows simultaneous reductions and provides a coherent understanding of these methods. To illustrate this idea, we begin with the form of (2.4). Denote $\bar{\boldsymbol{S}} \in \mathbb{R}^{p \times R_2 \times q}$ as a third-order tensor satisfying $\bar{\boldsymbol{S}}_{(2)} = \boldsymbol{D}^{\mathsf{T}}$. Model (2.4) can be written as

$$\boldsymbol{y} = \{\bar{\boldsymbol{S}} \, \bar{\times}_2 \, \boldsymbol{\beta}(t)\}^{\mathsf{T}} \boldsymbol{x} + \boldsymbol{\epsilon}, \tag{2.6}$$

where $\bar{\times}_2$ denotes the 2-mode (vector) product of a tensor with a vector (Kolda and Bader, 2009). More precisely, the result of the d-mode (vector) product of a generic Nth-order tensor $\mathfrak{G} = (g_{i_1, i_2, \ldots, i_N}) \in \mathbb{R}^{I_1 \times I_2 \times \cdots I_N}$ and a vector $\boldsymbol{v} \in \mathbb{R}^{I_d}$ is a tensor of order $N - 1$, with dimension $I_1 \times \cdots \times I_{d-1} \times I_{d+1} \times \cdots \times I_N$, such that its $(i_1, \ldots, i_{d-1}, i_{d+1}, \ldots, i_N)$th element is $\sum_{i_d=1}^{I_d} v_{i_d}$.

$g_{i_1,i_2,\ldots,i_N}$. This reformulation shows that exploring the correlations between the varying-coefficient

functions is equivalent to the dimension reduction on the second mode of a third-order tensor.

Figure 1 illustrates the corresponding matrix of coefficient functions in (2.6) using this tensor-

vector product. Similarly, the correlations between the predictors and the responses are related

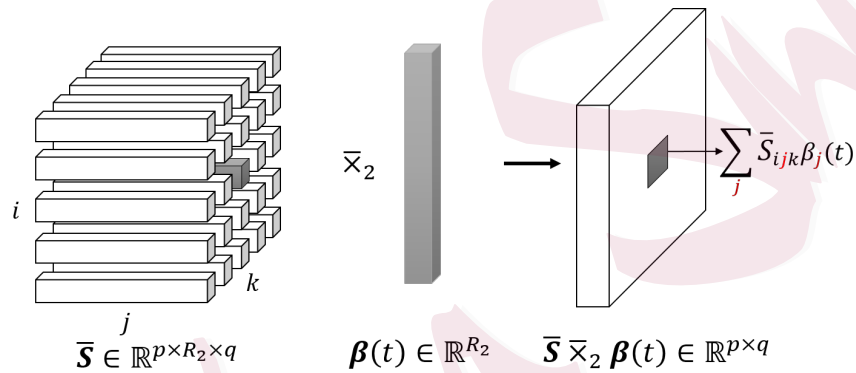to dimension reductions on the first and third modes, respectively.

Figure 1: An illustration plot of the coefficient functions matrix in (2.6) using a tensor formulation

and the 2-mode (vector) product.

Therefore, to simultaneously explore all reductions, we propose

$$\boldsymbol{y} = \{\boldsymbol{S} \times_1 \boldsymbol{A} \times_3 \boldsymbol{C} \,\bar{\times}_2\, \boldsymbol{\beta}(t)\} \,\bar{\times}_1\, \boldsymbol{x} + \boldsymbol{\epsilon}, \tag{2.7}$$

where $\times_d$ denotes the d-mode (matrix) product of a tensor with a matrix (Kolda and Bader,

2009), for $d = 1, 2, 3$; $\boldsymbol{\beta}(t)$ is a vector of R_2 unknown principal functions; and $\boldsymbol{S} \in \mathbb{R}^{R_1 \times R_2 \times R_3}$,

$\boldsymbol{A} \in \mathbb{R}^{p \times R_1}$, and $\boldsymbol{C} \in \mathbb{R}^{q \times R_3}$ are coefficients to be estimated. We depict $\boldsymbol{S} \times_1 \boldsymbol{A}$ in Figure 2 to

illustrate the d-mode (matrix) product of a tensor with a matrix. Similarly to Jiang et al. (2013),

Lian and Ma (2013), and He et al. (2018), we require $\boldsymbol{A}$, $\boldsymbol{C}$, and $\boldsymbol{\beta}(t)$ to be orthonormal, that is,

$$\boldsymbol{A}^\mathsf{T}\boldsymbol{A} = \boldsymbol{I}_{R_1}, \quad \boldsymbol{C}^\mathsf{T}\boldsymbol{C} = \boldsymbol{I}_{R_3}, \quad \text{and} \quad \int_{\mathcal{T}} \boldsymbol{\beta}(t)\boldsymbol{\beta}(t)^\mathsf{T}\, \mathrm{d}t = \boldsymbol{I}_{R_2}. \tag{2.8}$$
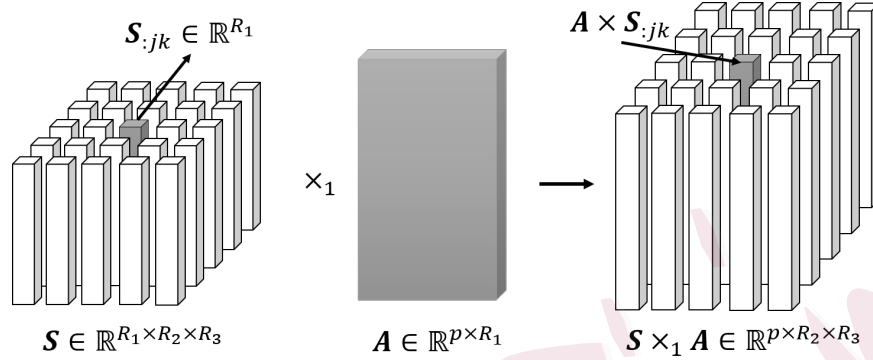
Figure 2: An illustration plot of the d-mode (matrix) product of a tensor and a matrix.

The multilinear structure of the varying coefficients $\boldsymbol{S} \times_1 \boldsymbol{A} \times_3 \boldsymbol{C} \ \bar{\times}_2 \boldsymbol{\beta}(t)$ coincides with the Tucker

decomposition (Tucker, 1966) for a third-order tensor. We observe that Models (2.3), (2.4), and

(2.5) are all special cases of Model (2.7). In particular, removing the first and second mode

reductions in (2.7) and writing $\boldsymbol{S} \times_1 \boldsymbol{A} \ \bar{\times}_2 \boldsymbol{\beta}(t) = \widetilde{\boldsymbol{F}}(t)$, (2.7) can recover (2.3). Furthermore, (2.4)

can be obtained directly by letting $\bar{\boldsymbol{S}} = \boldsymbol{S} \times_1 \boldsymbol{A} \times_3 \boldsymbol{C}$. Finally, singling out $\boldsymbol{A}$ and treating $q = 1$

in $\boldsymbol{S} \times_3 \boldsymbol{C} \ \bar{\times}_2 \boldsymbol{\beta}(t)$ recovers (2.5). Therefore, each mode in the decomposition $\boldsymbol{S} \times_1 \boldsymbol{A} \times_3 \boldsymbol{C} \ \bar{\times}_2 \boldsymbol{\beta}(t)$

corresponds to one of the aforementioned reduced models.

Note that the constraint (2.8) does not guarantee the identifiability of the proposed model

(2.7). Indeed for any $\boldsymbol{U} \in \mathbb{R}^{R_2 \times R_2}$ with $\boldsymbol{U}\boldsymbol{U}^\top = \boldsymbol{I}_{R_2}$, we have

$$\{\boldsymbol{S} \times_1 \boldsymbol{A} \times_3 \boldsymbol{C} \ \bar{\times}_2 \boldsymbol{\beta}(t)\}^\top \boldsymbol{x} = \left[(\boldsymbol{S} \times_2 \boldsymbol{U}) \times_1 \boldsymbol{A} \times_3 \boldsymbol{C} \ \bar{\times}_2 \{\boldsymbol{U}\boldsymbol{\beta}(t)\}\right]^\top \boldsymbol{x}.$$

In other words, $(\boldsymbol{S}, \boldsymbol{A}, \boldsymbol{C}, \boldsymbol{\beta}(t))$ and $(\boldsymbol{S} \times_2 \boldsymbol{U}, \boldsymbol{A}, \boldsymbol{C}, \boldsymbol{U}\boldsymbol{\beta}(t))$ result in the same reduced MVCM

model. However, we need only identify the regression coefficient functions $\boldsymbol{F}(t)$ to understand the

reduced MVCM (2.7), which is fulfilled, because $\boldsymbol{F}(t) = \boldsymbol{S} \times_1 \boldsymbol{A} \times_3 \boldsymbol{C} \ \bar{\times}_2 \boldsymbol{\beta}(t)$. In terms of com-

putation, these identifiability issues may lead to algorithmic instability. Therefore, we introduce

some further regularizations on $(\boldsymbol{S}, \boldsymbol{A}, \boldsymbol{C}, \boldsymbol{\beta}(t))$ in Section 3 to obtain an efficient algorithm.

3.   Penalized Least Squares Estimation

To estimate the parameters in our reduced MVCM (2.7), we first approximate the principal component functions $\boldsymbol{\beta}(t)$ using splines. Specifically, let $\boldsymbol{b}(t) = (b_1(t), \ldots, b_K(t))^\intercal$ be a vector of orthonormal B-spline basis functions with dimension K. For the r_2th principal component function $\beta_{r_2}(t)$, we write

$$\beta_{r_2}(t) \approx \sum_{k=1}^{K} B_{k,r_2} b_k(t),$$

where $\{B_{k,r_2}\}$ are the corresponding spline coefficients. Denote $\boldsymbol{B}_{r_2} = (B_{1,r_1}, \ldots, B_{K,r_2})^\intercal$. We stack $\boldsymbol{B}_{r_2}$, for $r_2 = 1, \ldots, R_2$, into a matrix of coefficients, and let $\boldsymbol{B} = (\boldsymbol{B}_1, \ldots, \boldsymbol{B}_{R_2}) \in \mathbb{R}^{K \times R_2}$. Moreover, we require $\boldsymbol{B}$ satisfies the constraint $\boldsymbol{B}^\intercal \boldsymbol{B} = \boldsymbol{I}_{R_2}$, which leads to the orthonormality of $\boldsymbol{\beta}(t)$ in (2.8). Ignoring the approximation error, Model (2.7) can then be written as

$$\begin{aligned}
\boldsymbol{y} &= \{\boldsymbol{S} \times_1 \boldsymbol{A} \,\bar{\times}_2\, \boldsymbol{B}^\intercal \boldsymbol{b}(t) \times_3 \boldsymbol{C}\}^\intercal \boldsymbol{x} + \boldsymbol{\epsilon} \\
&= \{\boldsymbol{S} \times_1 \boldsymbol{A} \times_2 \boldsymbol{B} \times_3 \boldsymbol{C} \,\bar{\times}_2\, \boldsymbol{b}(t)\}^\intercal \boldsymbol{x} + \boldsymbol{\epsilon}.
\end{aligned} \tag{3.1}$$

The above basis expansion enables us to recast the problem of estimating the varying coefficients of the reduced model (2.7) as that of estimating the parameters $(\boldsymbol{S}, \boldsymbol{A}, \boldsymbol{B}, \boldsymbol{C})$, where $\boldsymbol{S} \in \mathbb{R}^{R_1 \times R_2 \times R_3}$, $\boldsymbol{A} \in \mathbb{R}^{p \times R_1}$ with $\boldsymbol{A}^\intercal \boldsymbol{A} = \boldsymbol{I}_{R_1}$, $\boldsymbol{B} \in \mathbb{R}^{K \times R_2}$ with $\boldsymbol{B}^\intercal \boldsymbol{B} = \boldsymbol{I}_{R_2}$, and $\boldsymbol{C} \in \mathbb{R}^{q \times R_3}$ with $\boldsymbol{C}^\intercal \boldsymbol{C} = \boldsymbol{I}_{R_3}$. Given independent and identically distributed (i.i.d.) copies $\{(\boldsymbol{y}_i, \boldsymbol{x}_i, t_i)\}_{i=1}^{n}$ of $(\boldsymbol{y}, \boldsymbol{x}, t)$, we consider the constrained least squares estimator

$$\operatorname*{arg\,min}_{\boldsymbol{S}, \boldsymbol{A}, \boldsymbol{B}, \boldsymbol{C}} \sum_{i=1}^{n} \left\| \boldsymbol{y}_i - \{\boldsymbol{S} \times_1 \boldsymbol{A} \times_2 \boldsymbol{B} \times_3 \boldsymbol{C} \,\bar{\times}_2\, \boldsymbol{b}(t_i)\}^\intercal \boldsymbol{x}_i \right\|_2^2 \tag{3.2}$$

$$\text{s.t. } \boldsymbol{A}^\intercal \boldsymbol{A} = \boldsymbol{I}_{R_1}, \ \boldsymbol{B}^\intercal \boldsymbol{B} = \boldsymbol{I}_{R_2}, \ \boldsymbol{C}^\intercal \boldsymbol{C} = \boldsymbol{I}_{R_3}.$$

In (3.1) and (3.2), $\boldsymbol{S} \times_1 \boldsymbol{A} \times_2 \boldsymbol{B} \times_3 \boldsymbol{C}$ is the Tucker decomposition of a third-order tensor. In particular, letting $\boldsymbol{G} = \boldsymbol{S} \times_1 \boldsymbol{A} \times_2 \boldsymbol{B} \times_3 \boldsymbol{C}$, we have $\text{rank}_1(\boldsymbol{G}) \leq R_1$, $\text{rank}_2(\boldsymbol{G}) \leq R_2$,

and $\text{rank}_3(\boldsymbol{G}) \leq R_3$, where $\text{rank}_d(\cdot)$ denotes the d-rank of a tensor (Kolda and Bader, 2009),

for $d = 1, 2, 3$. We depict the Tucker decomposition representation of model (3.1) in Figure

3. For further discussions on the Tucker decomposition and its relationship with other tensor

decompositions, such as the CANDECOMP/PARAFAC (CP) decomposition (Harshman, 1970)

and tensor-train decomposition (Oseledets, 2011), we refer the readers to Kolda and Bader (2009).

Using the form of the Tucker decomposition, the least squares problem (3.2) is equivalent to

$$\arg\min_{\boldsymbol{G}} \sum_{i=1}^{n} \left\| \boldsymbol{y}_i - \{\boldsymbol{G} \ \bar{\times}_2 \ \boldsymbol{b}(t_i)\}^{\mathsf{T}} \boldsymbol{x}_i \right\|_2^2 \quad \text{s.t.} \quad \text{rank}_d(\boldsymbol{G}) \leq R_d, \ d = 1, 2, 3. \tag{3.3}$$

The benefits of using a low-rank structure in tensor regression models rather than simply flattening

the covariate tensor to a matrix or a vector are discussed in Zhou et al. (2013), Li et al. (2018),

and Ahmed et al. (2020). Note that our problem is different from those in existing works on the

Tucker tensor regression (Li et al., 2018) and its generalizations (Lu et al., 2020; Ahmed et al.,

2020) in two aspects. First, (3.1) is *not* the proposed model, but merely an approximation of the

target *nonparametric* model (2.7). Second, we study a multivariate response $\boldsymbol{y}$, whereas Li et al.

(2018); Lu et al. (2020); Ahmed et al. (2020) all assume the response variable is a scalar.

For a large value of pq, the dimension reduction in terms of a low-rank Tucker decomposition

may not lead to an accurate estimation for the varying coefficients. Many applications expect

the responses to have similar/related structures, and thus share many important predictors.

Furthermore, the union of these important predictors usually has a small size. In other words, we

assume that only s ($s < p$ and unknown) predictors are relevant for predicting all the responses.

This assumption is shown to be suitable for many real-world applications; see, for example,

Wang et al. (2008); Wei et al. (2011) and He et al. (2018), among many others. We use a

sparsity-inducing penalization to filter out the irrelevant predictors during the estimation. To
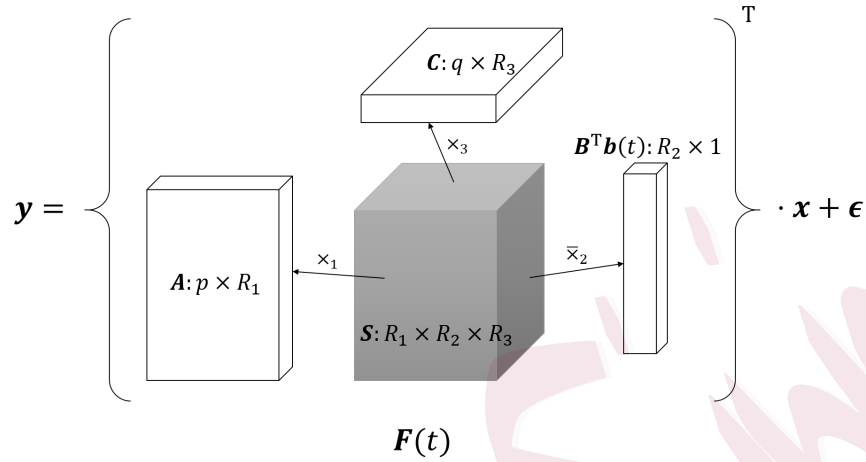
Figure 3: The Tucker decomposition representation of model (3.1).

formulate a suitable penalty function, we use the Tucker decomposition $\boldsymbol{G} = \boldsymbol{S} \times_1 \boldsymbol{A} \times_2 \boldsymbol{B} \times_3 \boldsymbol{C}$

again, and rewrite (3.1) as

$$\boldsymbol{y} = \{\boldsymbol{G} \,\bar{\times}_2\, \boldsymbol{b}(t)\}^{\mathsf{T}} \boldsymbol{x} + \boldsymbol{\epsilon} = \{\boldsymbol{I}_q \otimes \boldsymbol{b}(t)^{\mathsf{T}}\} \boldsymbol{G}_{(1)}^{\mathsf{T}} \boldsymbol{x} + \boldsymbol{\epsilon}, \tag{3.4}$$

where $\boldsymbol{G}_{(1)} \in \mathbb{R}^{p \times qK}$ is the mode-1 matricization (unfolding) of tensor $\boldsymbol{G}$, and $\otimes$ is the Kronecker

product of matrices (Kolda and Bader, 2009). Let $\boldsymbol{G}_{(1),j}^{\mathsf{T}}$ denote the jth row of $\boldsymbol{G}_{(1)}$, for $j =$

$1, \ldots, p$. In light of (3.4), all unknown coefficients associated with the jth predictor are contained

in $\boldsymbol{G}_{(1),j}^{\mathsf{T}}$. Therefore, the jth predictor becomes irrelevant whenever the coefficient matrix $\boldsymbol{G}_{(1),j}^{\mathsf{T}} =$

$\boldsymbol{0}$. Borrowing the idea from the group lasso penalization (Yuan and Lin, 2006), we propose the

following penalized least squares problem:

$$\arg\min_{\boldsymbol{G}} \sum_{i=1}^{n} \left\| \boldsymbol{y}_i - \{\boldsymbol{G} \,\bar{\times}_2\, \boldsymbol{b}(t_i)\}^{\mathsf{T}} \boldsymbol{x}_i \right\|_2^2 + \sum_{j=1}^{p} \lambda \|\boldsymbol{G}_{(1),j}\|_2, \text{ s.t. } \mathrm{rank}_d(\boldsymbol{G}) \le R_d, \ d = 1, 2, 3, \tag{3.5}$$

where $\| \cdot \|_2$ is the group lasso penalty, and $\lambda \ge 0$ is the penalty parameter. Note that $\boldsymbol{G}_{(1)} =$

$\boldsymbol{A} \boldsymbol{S}_{(1)} (\boldsymbol{C} \otimes \boldsymbol{B})^{\mathsf{T}}$. Let $\boldsymbol{a}_j^{\mathsf{T}}$ be the jth row of $\boldsymbol{A}$. Then, $\boldsymbol{G}_{(1),j}^{\mathsf{T}} = \boldsymbol{a}_j^{\mathsf{T}} \boldsymbol{S}_{(1)} (\boldsymbol{C} \otimes \boldsymbol{B})^{\mathsf{T}}$. Due to the

orthonormal conditions of $\boldsymbol{B}$ and $\boldsymbol{C}$, we have $\|\boldsymbol{G}_{(1),j}\|_2 = \|\boldsymbol{a}_j^{\mathsf{T}}\boldsymbol{S}_{(1)}(\boldsymbol{C} \otimes \boldsymbol{B})^{\mathsf{T}}\|_2 = \|\boldsymbol{a}_j^{\mathsf{T}}\boldsymbol{S}_{(1)}\|_2$.

Therefore, (3.5) is equivalent to

$$
\underset{\boldsymbol{S},\boldsymbol{A},\boldsymbol{B},\boldsymbol{C}}{\arg\min} \sum_{i=1}^n \left\|\boldsymbol{y}_i - \{\boldsymbol{S} \times_1 \boldsymbol{A} \times_2 \boldsymbol{B} \times_3 \boldsymbol{C} \bar{\times}_2 \boldsymbol{b}(t_i)\}^{\mathsf{T}}\boldsymbol{x}_i\right\|_2^2 + \sum_{j=1}^p \lambda\|\boldsymbol{a}_j^{\mathsf{T}}\boldsymbol{S}_{(1)}\|_2 \tag{3.6}
$$

$$
\text{s.t. } \boldsymbol{A}^{\mathsf{T}}\boldsymbol{A} = \boldsymbol{I}_{R_1}, \ \boldsymbol{B}^{\mathsf{T}}\boldsymbol{B} = \boldsymbol{I}_{R_2}, \ \boldsymbol{C}^{\mathsf{T}}\boldsymbol{C} = \boldsymbol{I}_{R_3}.
$$

Let $(\widehat{\boldsymbol{S}}, \widehat{\boldsymbol{A}}, \widehat{\boldsymbol{B}}, \widehat{\boldsymbol{C}})$ be a solution of (3.6). Correspondingly, a solution of (3.5) can be constructed

as $\widehat{\boldsymbol{G}} = \widehat{\boldsymbol{S}} \times_1 \widehat{\boldsymbol{A}} \times_2 \widehat{\boldsymbol{B}} \times_3 \widehat{\boldsymbol{C}}$ (or, equivalently, $\widehat{\boldsymbol{G}}_{(1)} = \widehat{\boldsymbol{A}}\widehat{\boldsymbol{S}}_{(1)}(\widehat{\boldsymbol{C}} \otimes \widehat{\boldsymbol{B}})^{\mathsf{T}}$). The resulting estimated

$f_{jl}(t)$ becomes

$$
\widehat{f}_{jl}(t) = \sum_{k=1}^K \widehat{G}_{jkl}b_k(t), \tag{3.7}
$$

where $\widehat{G}_{jkl}$ is the (j,k,l)th element of $\widehat{\boldsymbol{G}}$. We provide a theoretical analysis of the proposed

estimation in Section 5.

4. Computation

To calculate the estimator, we propose a block updating algorithm to solve the problem given in

(3.6), that is, updating $\boldsymbol{S}$, $\boldsymbol{A}$, $\boldsymbol{B}$, and $\boldsymbol{C}$ alternately while keeping the other components fixed.

To facilitate the discussion, we let $\mathcal{L}(\boldsymbol{S},\boldsymbol{A},\boldsymbol{B},\boldsymbol{C})$ be the objective function in (3.6) for a given λ,

and denote the squared loss and the penalty by

$$
H(\boldsymbol{S},\boldsymbol{A},\boldsymbol{B},\boldsymbol{C}) = \sum_{i=1}^n \left\|\boldsymbol{y}_i - \{\boldsymbol{S} \times_1 \boldsymbol{A} \times_2 \boldsymbol{B} \times_3 \boldsymbol{C} \bar{\times}_2 \boldsymbol{b}(t_i)\}^{\mathsf{T}}\boldsymbol{x}_i\right\|_2^2 \text{ and } P(\boldsymbol{S},\boldsymbol{A}) = \sum_{j=1}^p \lambda\|\boldsymbol{a}_j^{\mathsf{T}}\boldsymbol{S}_{(1)}\|_2,
$$

respectively. Denote $\boldsymbol{S}^{(t)}, \boldsymbol{A}^{(t)}, \boldsymbol{B}^{(t)}$, and $\boldsymbol{C}^{(t)}$ as the tth iteration $(t \geq 1)$ of $\boldsymbol{S}$, $\boldsymbol{A}$, $\boldsymbol{B}$, and $\boldsymbol{C}$,

respectively, in the proposed algorithm. When we update one block with the other blocks fixed,

we use H and/or P with suitable subscripts to simplify the objective functions with respect to

the target block. For example, when $\boldsymbol{A}^{(t)}$, $\boldsymbol{B}^{(t)}$, and $\boldsymbol{C}^{(t)}$ are fixed, we let $H_{\boldsymbol{A}^{(t)},\boldsymbol{B}^{(t)},\boldsymbol{C}^{(t)}}(\boldsymbol{S}) = H(\boldsymbol{S},\boldsymbol{A}^{(t)},\boldsymbol{B}^{(t)},\boldsymbol{C}^{(t)})$ and $P_{\boldsymbol{A}^{(t)}}(\boldsymbol{S}) = P(\boldsymbol{S},\boldsymbol{A}^{(t)})$ be the functions with respect to $\boldsymbol{S}$. Analogously, we have $H_{\boldsymbol{S}^{(t+1)},\boldsymbol{B}^{(t)},\boldsymbol{C}^{(t)}}(\boldsymbol{A})$, $H_{\boldsymbol{S}^{(t+1)},\boldsymbol{A}^{(t+1)},\boldsymbol{C}^{(t)}}(\boldsymbol{B})$, and $P_{\boldsymbol{S}^{(t+1)}}(\boldsymbol{A})$. The details for each block are discussed in the following subsections.

4.1 Updating $\boldsymbol{S}$

Using the properties of vectorization (unfolding of a tensor) and the d-mode (matrix) product (Kolda and Bader, 2009), we can rewrite $H_{\boldsymbol{A}^{(t)},\boldsymbol{B}^{(t)},\boldsymbol{C}^{(t)}}(\boldsymbol{S})$ and $P_{\boldsymbol{A}^{(t)}}(\boldsymbol{S})$ as

$$H_{\boldsymbol{A}^{(t)},\boldsymbol{B}^{(t)},\boldsymbol{C}^{(t)}}(\boldsymbol{S}) = \sum_{i=1}^{n} \|\boldsymbol{y}_i - [\boldsymbol{C}^{(t)} \otimes \{\boldsymbol{b}^{\intercal}(t_i)\boldsymbol{B}^{(t)}\} \otimes (\boldsymbol{x}_i^{\intercal}\boldsymbol{A}^{(t)})]\mathrm{vec}\{\boldsymbol{S}_{(1)}\}\|_2^2$$

$$\text{and} \quad P_{\boldsymbol{A}^{(t)}}(\boldsymbol{S}) = \lambda \sum_{j=1}^{p} \|(\boldsymbol{a}_j^{(t)})^{\intercal}\boldsymbol{S}_{(1)}\|_2,$$

respectively, where $\boldsymbol{S}_{(1)} \in \mathbb{R}^{R_1 \times R_2 R_3}$ is the mode-1 matricization (unfolding) of the tensor $\boldsymbol{S}$, $\mathrm{vec}(\cdot)$ is the vectorization operator, and $(\boldsymbol{a}_j^{(t)})^{\intercal}$ is the jth row of $\boldsymbol{A}^{(t)}$. Thus, updating $\boldsymbol{S}$ is equivalent to obtaining the solution of

$$\min_{\boldsymbol{S} \in \mathbb{R}^{R_1 \times R_2 \times R_3}} H_{\boldsymbol{A}^{(t)},\boldsymbol{B}^{(t)},\boldsymbol{C}^{(t)}}(\boldsymbol{S}) + P_{\boldsymbol{A}^{(t)}}(\boldsymbol{S}). \tag{4.1}$$

Because $P_{\boldsymbol{A}^{(t)}}(\boldsymbol{S})$ is not differentiable, we propose using a majorization-minimization (MM) algorithm. The acronym can also stand for minorization-maximization if one aims to find the maximum of an objective function; see, for example, Hunter and Lange (2004). MM algorithms are useful extensions of the well-known class of EM algorithms, in which the E-step is equivalent to a minorization step. To construct the majorized function for $P_{\boldsymbol{A}^{(t)}}(\boldsymbol{S})$, we extend the MM algorithm of the lasso penalty (Hunter and Li, 2005) to the group lasso penalization. Moreover,

since (4.1) is an objective function with respect to a tensor, some tensor operations need to be considered and applied to this subproblem. See Section S.1.1 of the Supplementary Material for more details, where Algorithm S.1 summarizes the proposed MM algorithm to update $\boldsymbol{S}$.

4.2 Updating $\boldsymbol{A}$

Similarly to Section 4.1, we use the properties of vectorization and the d-mode (matrix) product (Kolda and Bader, 2009) to rewrite $H_{\widetilde{\boldsymbol{S}}^{(t+1)}, \boldsymbol{B}^{(t)}, \boldsymbol{C}^{(t)}}(\boldsymbol{A})$ as

$$H_{\widetilde{\boldsymbol{S}}^{(t+1)}, \boldsymbol{B}^{(t)}, \boldsymbol{C}^{(t)}}(\boldsymbol{A}) = \frac{1}{2} \sum_{i=1}^{n} \left\| \boldsymbol{y}_i - \left[\left\{ \left[\boldsymbol{C}^{(t)} \otimes \{ \boldsymbol{b}^{\intercal}(t_i) \boldsymbol{B}^{(t)} \} \right] \big(\widetilde{\boldsymbol{S}}_{(1)}^{(t+1)} \big)^{\intercal} \right\} \otimes \boldsymbol{x}_i^{\intercal} \right] \mathrm{vec}(\boldsymbol{A}) \right\|^2.$$

To simplify the updating procedure for $\boldsymbol{A}$, we first remove the orthonormal constraint on $\boldsymbol{A}$ and update $\boldsymbol{A}$ in the Euclidean space. An orthonormalization step is added in the outer loop to project the updated $\boldsymbol{A}$ back to an orthonormal matrix. The subproblem of $\boldsymbol{A}$ without the orthonormal constraint can then be written as

$$\min_{\boldsymbol{A}} \left\{ H_{\widetilde{\boldsymbol{S}}^{(t+1)}, \boldsymbol{B}^{(t)}, \boldsymbol{C}^{(t)}}(\boldsymbol{A}) + P_{\boldsymbol{S}^{(t+1)}}(\boldsymbol{A}) \right\}, \tag{4.2}$$

where $P_{\boldsymbol{S}^{(t+1)}}(\boldsymbol{A}) = \lambda \sum_{j=1}^{p} \| (\widetilde{\boldsymbol{S}}_{(1)}^{(t+1)})^{\intercal} \boldsymbol{a}_j \|$. Because there is no analytic solution to (4.2), we propose using the ADMM (Gabay and Mercier, 1976). Denote $g(x) = \|x\|$ and introduce the slack variable $\gamma_j \in \mathbb{R}^{R_2 R_3}$, for $j = 1, \ldots, p$. We rewrite the optimization problem (4.2) as

$$\min_{\boldsymbol{A}, \boldsymbol{\Gamma}} \left\{ H_{\widetilde{\boldsymbol{S}}^{(t+1)}, \boldsymbol{B}^{(t)}, \boldsymbol{C}^{(t)}}(\boldsymbol{A}) + \lambda \sum_{j=1}^{p} g(\boldsymbol{\gamma}_j) \right\}, \quad \text{s.t.} \quad \boldsymbol{\Gamma} = \boldsymbol{A} \widetilde{\boldsymbol{S}}_{(1)}^{(t+1)}, \tag{4.3}$$

where $\boldsymbol{\Gamma} = (\boldsymbol{\gamma}_1, \boldsymbol{\gamma}_2, \ldots, \boldsymbol{\gamma}_p)^{\intercal}$. In (4.3), the constraint is equivalent to $\boldsymbol{\gamma}_j = (\widetilde{\boldsymbol{S}}_{(1)}^{(t+1)})^{\intercal} \boldsymbol{a}_j$, for $j = 1, 2, \ldots, p$. The corresponding augmented Lagrangian function is

$$\mathcal{L}_\rho(\boldsymbol{A}, \boldsymbol{\Gamma}; \boldsymbol{\nu}) = H_{\widetilde{\boldsymbol{S}}^{(t+1)}, \boldsymbol{B}^{(t)}, \boldsymbol{C}^{(t)}}(\boldsymbol{A}) + \lambda \sum_{j=1}^{p} g(\boldsymbol{\gamma}_j) + \frac{\rho}{2} \left\| \boldsymbol{A} \widetilde{\boldsymbol{S}}_{(1)}^{(t+1)} - \boldsymbol{\Gamma} + \frac{1}{\rho} \boldsymbol{\nu} \right\|_2^2, \tag{4.4}$$

where $\boldsymbol{\nu} \in \mathbb{R}^{p \times R_2 R_3}$ is the dual variable.

We defer the detailed analysis of (4.4) to Section S.1.2 of the Supplementary Material, in which Algorithm S.2 summarizes the proposed ADMM algorithm. Let $\widetilde{\boldsymbol{A}}^{(t+1)}$ denote the output of Algorithm S.2 for $\boldsymbol{A}$. To project $\widetilde{\boldsymbol{A}}^{(t+1)}$ onto the space of orthonormal matrices, we further let qr.Q($\widetilde{\boldsymbol{A}}^{(t+1)}$) and qr.R($\widetilde{\boldsymbol{A}}^{(t+1)}$) be the Q and R factors of the QR decomposition of $\widetilde{\boldsymbol{A}}^{(t+1)}$, respectively. Here, we require the R factor to have positive diagonal elements for the QR identifiability. We update $\boldsymbol{A}^{(t+1)}$ as qr.Q($\widetilde{\boldsymbol{A}}^{(t+1)}$), and then update $\boldsymbol{S}_{(1)}^{(t+1)}$ as qr.R($\widetilde{\boldsymbol{A}}^{(t+1)}$) $\cdot \widetilde{\boldsymbol{S}}_{(1)}^{(t+1)}$. By using the inverse of the mode-1 unfolding on $\boldsymbol{S}_{(1)}^{(t+1)}$, $\boldsymbol{S}^{(t+1)}$ is also obtained. Note that the direct output of Algorithm S.2 does not result in the exact row sparsity of $\widetilde{\boldsymbol{A}}^{(t+1)} \widetilde{\boldsymbol{S}}_{(1)}^{(t+1)}$. To select the variables in our algorithm, we output the slack variable $\boldsymbol{\Gamma}^{(t+1)}$ in Algorithm S.2 as an auxiliary result, and replace $\widetilde{\boldsymbol{A}}^{(t+1)} \widetilde{\boldsymbol{S}}_{(1)}^{(t+1)}$ with $\boldsymbol{\Gamma}^{(t+1)}$. Due to the constraint of the slack variable in (4.3), the difference between these two terms is sufficiently small. The output of $\boldsymbol{\Gamma}^{(t+1)}$ in Algorithm S.2 remains unchanged after applying the above orthonormalization step.

4.3 Updating $\boldsymbol{B}$

We let the orthogonal Stiefel manifold be

$$\mathrm{St}(R_2, K) = \{\boldsymbol{B} \in \mathbb{R}^{K \times R_2} : \boldsymbol{B}^\intercal \boldsymbol{B} = \boldsymbol{I}_{R_2}\}. \tag{4.5}$$

Using the properties of the d-mode product of a tensor and a matrix (Kolda and Bader, 2009), we can rewrite $H_{\boldsymbol{S}^{(t+1)}, \boldsymbol{A}^{(t+1)}, \boldsymbol{C}^{(t)}}(\boldsymbol{B})$, and update $\boldsymbol{B}$ from solving the optimization problem

$$\boldsymbol{B}^{(t+1)} = \underset{\boldsymbol{B} \in \mathrm{St}(R_2, K)}{\arg\min} \sum_{i=1}^{n} \left\| \boldsymbol{y}_i - ([\{\boldsymbol{C}^{(t)} \otimes (\boldsymbol{x}_i^\intercal \boldsymbol{A}^{(t+1)})\}\{\boldsymbol{S}_{(2)}^{(t+1)}\}^\intercal] \otimes \boldsymbol{b}^\intercal(t_i))\mathrm{vec}(\boldsymbol{B}) \right\|_2^2, \tag{4.6}$$

where $\boldsymbol{S}_{(2)}$ is the mode-2 matricization of tensor $\boldsymbol{S}$. Note that the objective function in (4.6) is a smooth function with respect to $\boldsymbol{B}$ on the Stiefel manifold (4.5), so we can use the manifold gradient method (Absil et al., 2009), which is an extension of the gradient descent algorithm to the manifold space. Algorithm S.3 in Section S.1.3 of the Supplementary Material specializes our implementation to use the gradient descent algorithm on the Stiefel manifold.

4.4 Updating $\boldsymbol{C}$

Using $\boldsymbol{S}_{(3)}$ as the mode-3 matricization (unfolding) of tensor $\boldsymbol{S}$, we can rewrite (3.1) as

$$\boldsymbol{y} = \boldsymbol{C}\boldsymbol{S}_{(3)}\{(\boldsymbol{b}^{\mathsf{T}}(t)\boldsymbol{B}) \otimes (\boldsymbol{x}^{\mathsf{T}}\boldsymbol{A})\}^{\mathsf{T}} + \boldsymbol{\epsilon}.$$

Denote $\boldsymbol{Y} = (\boldsymbol{y}_1, \dots, \boldsymbol{y}_n)^{\mathsf{T}} \in \mathbb{R}^{n \times q}$ and $\boldsymbol{M}_C^{(t)} = (\boldsymbol{M}_{C,1}^{(t)}, \dots, \boldsymbol{M}_{C,n}^{(t)})^{\mathsf{T}} \in \mathbb{R}^{n \times R_3}$, where $\boldsymbol{M}_{C,i}^{(t)} = \{\boldsymbol{b}^{\mathsf{T}}(t_i)\boldsymbol{B}^{(t+1)} \otimes (\boldsymbol{x}_i^{\mathsf{T}}\boldsymbol{A}^{(t+1)})\}(\boldsymbol{S}_{(3)}^{(t+1)}) \in \mathbb{R}^{R_3}$, for $i = 1, \dots, n$. We then focus the following subproblem to update $\boldsymbol{C}$:

$$\boldsymbol{C}^{(t+1)} = \underset{\boldsymbol{C}^{\mathsf{T}}\boldsymbol{C}=\boldsymbol{I}}{\arg\min} \left\|\boldsymbol{Y} - \boldsymbol{M}_C^{(t)}\boldsymbol{C}^{\mathsf{T}}\right\|_F^2, \tag{4.7}$$

which is known as the orthonormal Procrustes problem (Gower and Dijksterhuis, 2004). Fining the solution to this problem is equivalent to determining the nearest orthonormal matrix of $\boldsymbol{Y}^{\mathsf{T}}\boldsymbol{M}_C^{(t)}$. Therefore, write the singular value decomposition of $\boldsymbol{Y}^{\mathsf{T}}\boldsymbol{M}_C^{(t)}$ as

$$\boldsymbol{Y}^{\mathsf{T}}\boldsymbol{M}_C^{(t)} = \boldsymbol{U}\boldsymbol{\Sigma}\boldsymbol{V}^{\mathsf{T}}, \tag{4.8}$$

where $\boldsymbol{U} \in \mathbb{R}^{q \times R_3}$ and $\boldsymbol{V} \in \mathbb{R}^{R_3 \times R_3}$ are orthonormal matrices, and $\boldsymbol{\Sigma} \in \mathbb{R}^{R_3 \times R_3}$ is a diagonal matrix with nonnegative values in its diagonal. The analytic solution to (4.7) can be obtained as

$$\boldsymbol{C}^{(t+1)} = \boldsymbol{U}\boldsymbol{V}^{\mathsf{T}}. \tag{4.9}$$

4.5 Summary and Initializations

Here, we summarize the block updating algorithm in Algorithm 1. To achieve a sparse solution, the output of Algorithm 1 is $\widehat{\boldsymbol{G}}_{(1)} = \widehat{\boldsymbol{\Gamma}}(\widehat{\boldsymbol{C}} \otimes \widehat{\boldsymbol{B}})^\intercal$. We can then reconstruct $\widehat{\boldsymbol{G}}$ from the estimated $\widehat{\boldsymbol{G}}_{(1)}$ by using the inverse of the mode-1 unfolding, and obtain the estimator of the varying coefficients using (3.7).

For the subproblems of $\boldsymbol{S}$ and $\boldsymbol{A}$, owing to convexity, we can show that the corresponding MM algorithm generates a sequence converging to the unique minimizer of each subproblem, using similar arguments to those for Corollary 3.3 of Hunter and Li (2005). We thus use random initializations for $\boldsymbol{S}$ and $\boldsymbol{A}$ at the first iteration of the outer loop. Then, we set the outputs of $\boldsymbol{S}$ and $\boldsymbol{A}$ from the preceding iteration of the outer loop as the initialization values for the next iteration of the outer loop. For $\boldsymbol{C}$, the corresponding subproblem for this component can be written as an orthogonal Procrustes problem that has a closed-form solution and, thus, no initialization is needed for $\boldsymbol{C}$. Finally, the subproblem for $\boldsymbol{B}$ is not convex due to the orthonormal constraint, and the proposed manifold gradient descent algorithm uses only the first-order information on the objective function, which may not guarantee the convergence to a local minimizer (Absil et al., 2009). Therefore, although Algorithm 1 can guarantee a sequence of decreasing values of the objective function, it is unclear whether this algorithm can guarantee the convergence to a global minimizer. Nevertheless, Absil et al. (2009) show that using any sub-sequence of the iterations generated by the manifold gradient descent algorithm converges to the stationary point of the subproblem. We can thus run Algorithm 1 from multiple initializations of $\boldsymbol{B}$ and return the best result. However, this is computationally expensive. Instead, we propose using a rough estimator $\boldsymbol{B}^{\text{init}}$ as an initial point for the manifold optimization of $\boldsymbol{B}$. Specifically, at the $(t+1)$th iteration,

define

$$\widetilde{\boldsymbol{B}} := \underset{\boldsymbol{B} \in \mathbb{R}^{K \times R_2}}{\arg \min} \, H_{\boldsymbol{S}^{(t+1)}, \boldsymbol{A}^{(t+1)}, \boldsymbol{C}^{(t)}}(\boldsymbol{B}),$$

which can be solved easily, since the objective function is differentiable with respect to $\boldsymbol{B}$ in the Euclidean space. Next, we simply project $\widetilde{\boldsymbol{B}}$ onto the Stiefel manifold, and let the projection be the initial point, that is,

$$\boldsymbol{B}^{\text{init}} = \mathcal{P}_{\text{St}(R_2, K)}(\widetilde{\boldsymbol{B}}) = \widetilde{\boldsymbol{B}}(\widetilde{\boldsymbol{B}}^{\intercal} \widetilde{\boldsymbol{B}})^{-1/2}.$$

We use the above $\boldsymbol{B}^{\text{init}}$ as the initial value in Algorithm S.3 when we update $\boldsymbol{B}$. Our numerical experiments show that this strategy is not only faster than using multiple random initializations but also generates stable iteration sequences.

4.6   Tuning Parameters

Our model has a total of six tuning parameters $(m, K, R_1, R_2, R_3, \lambda)$, where m is the order of the spline basis, K is the number of basis functions, (R_1, R_2, R_3) are the Tucker ranks, and λ is the regularization parameter. We first fix the spline order $m = 4$ (cubic spline) to alleviate the computational burden of estimating nonparametric functions (Ruppert et al., 2003). For the number K of spline basis functions, many data-driven methods have been proposed to decide K based on the sample size (see, e.g., Huang et al., 2002, 2004; Ruppert et al., 2003, and the references therein) in empirical studies. To be computationally simple, we follow the strategy used in Fan et al. (2014) by letting $K = [2n^{1/5}]$, where $[\cdot]$ denotes rounding to the nearest integer. The knots of spline basis functions are also data-driven, and chosen as equally spaced quantiles. We find this empirical rule works well in all of our experiments. For the choice of R_3, which corresponds to the dimension reduction associated with the responses, we conduct a singular

---

Algorithm 1: Block Updating Algorithm to Solve (3.6).

   Input: Data set $\{\boldsymbol{y}_i, \boldsymbol{X}_i, t_i\}_{i=1}^n$; Random initial points

$$\boldsymbol{S}^{(0)} \in \mathbb{R}^{R_1 \times R_2 \times R_3}, \boldsymbol{A}^{(0)} \in \mathbb{R}^{p \times R_1}, \boldsymbol{B}^{(0)} \in \text{St}(R_2, K), \boldsymbol{C}^{(0)} \in \text{St}(R_3, q), \text{ and } t = 0.$$

   Output: $\widehat{\boldsymbol{G}}_{(1)} = \widehat{\boldsymbol{\Gamma}}(\widehat{\boldsymbol{C}} \otimes \widehat{\boldsymbol{B}})^{\intercal}.$

   repeat

        1. Update $\widetilde{\boldsymbol{S}}^{(t+1)}$ using Algorithm S.1.

        2. Update $\widetilde{\boldsymbol{A}}^{(t+1)}$ using Algorithm S.2 and $\boldsymbol{\Gamma}^{(t+1)}$ for variable selection.

        3. After the QR decomposition of $\widetilde{\boldsymbol{A}}^{(t+1)}$, let $\boldsymbol{A}^{(t+1)}$ and $\boldsymbol{S}_{(1)}^{(t+1)}$ be qr.Q$(\widetilde{\boldsymbol{A}}^{(t+1)})$ and

           qr.R$(\widetilde{\boldsymbol{A}}^{(t+1)}) \cdot \widetilde{\boldsymbol{S}}_{(1)}^{(t+1)}$, repectively.

        4. Update $\boldsymbol{B}^{(t+1)}$ using the manifold gradient descent method (Algorithm S.3).

        5. Update $\boldsymbol{C}^{(t+1)} = \boldsymbol{U}\boldsymbol{V}^{\intercal}$ as in (4.9), with $\boldsymbol{U}$ and $\boldsymbol{V}$ defined in (4.8).

        6. $t = t + 1$.

   until $\mathcal{L}(\boldsymbol{S}^{(t+1)}, \boldsymbol{A}^{(t+1)}, \boldsymbol{B}^{(t+1)}, \boldsymbol{C}^{(t+1)}) - \mathcal{L}(\boldsymbol{S}^{(t)}, \boldsymbol{A}^{(t)}, \boldsymbol{B}^{(t)}, \boldsymbol{C}^{(t)}) < \epsilon$. Denote $\widehat{\boldsymbol{\Gamma}} = \boldsymbol{\Gamma}^{(t+1)}$,

   $\widehat{\boldsymbol{C}} = \boldsymbol{C}^{(t+1)}$, and $\widehat{\boldsymbol{B}} = \boldsymbol{B}^{(t+1)}$.

---

value decomposition of the response matrix $\boldsymbol{Y} \in \mathbb{R}^{n \times q}$. We then choose R_3 such that the first

R_3 dominant singular values together account for at least 90% of the sum of all singular values.

For (R_1, R_2) and λ, we apply the hold-out method (He et al., 2018; Hannun et al., 2019) in our

numerical study, for its computational efficiency. More precisely, we randomly split the available

data into two subsets: a training set with 75% of the samples, and a validation set with 25% of

the samples. We set the validation samples aside, and use Algorithm 1 to fit our proposed method

on the training set. The parameters (R_1, R_2) and λ are selected by minimizing the validation

error

$$\frac{1}{n_{\text{valid}}} \sum_{i=1}^{n_{\text{valid}}} (y_{\text{valid},i} - \widehat{y}_{\text{valid},i})^2$$

over the grids of the corresponding tuning parameters, where n_{valid} is the size of the validation

set, and $\widehat{y}_{\text{valid},i}$ is the prediction value of the ith observation $y_{\text{valid},i}$ in the validation set.

5. Theory

In this section, we establish the oracle inequality for the prediction accuracy of the proposed

estimator. For readability, we first show the oracle inequality under a *fixed-design* setting, where

the predictors and the exposure variable are fixed. Similarly, we say a setting is *random-design*

if these variables are distributed randomly. To extend our results to random-design settings, we

show that the corresponding assumption on the design (that is, Condition $\mathcal{M}(\mathcal{J}, \delta_{\mathcal{J}})$ presented

below) can be satisfied with high probability (tending to one) when $\boldsymbol{x}$ and t are random, under

some mild regularity conditions. The result under the fixed-design setting is presented below; we

defer the theoretical result for the random design to Section S.4 of the Supplementary Material.

Let $\boldsymbol{\Sigma} = \boldsymbol{Z}^{\mathsf{T}}\boldsymbol{Z}/n$, $\boldsymbol{Z} = (\boldsymbol{z}_1, \ldots, \boldsymbol{z}_n)^{\mathsf{T}}$, where $\boldsymbol{z}_i = \boldsymbol{x}_i \otimes \boldsymbol{b}(t_i) \in \mathbb{R}^{pK}$. We use $\lambda_{\max}(\cdot)$ and

$\lambda_{\min}(\cdot)$ to denote the maximum and minimum eigenvalues of a matrix, respectively. Denote

by $\boldsymbol{S}_0$, $\boldsymbol{A}_0$, $\boldsymbol{C}_0$, and $\boldsymbol{\beta}_0$ the true values of $\boldsymbol{S}$, $\boldsymbol{A}$, $\boldsymbol{C}$, and $\boldsymbol{\beta}$ in (2.7), respectively. Denote by

s the number of nonzero rows in $\boldsymbol{A}_0$, which corresponds to the relevant predictors. We also

write $\boldsymbol{H}_0 = \boldsymbol{S}_0 \times_1 \boldsymbol{A}_0 \times_3 \boldsymbol{C}_0 \in \mathbb{R}^{p \times R_2 \times q}$, and correspondingly, the true coefficient functions are

$(f_{0,jl}(t))_{p \times q} = \boldsymbol{F}_0(t) = \boldsymbol{H}_0 \bar{\times}_2 \boldsymbol{\beta}_0(t)$. Let

$$\boldsymbol{Y} = (\boldsymbol{y}_1, \ldots, \boldsymbol{y}_n)^{\mathsf{T}} \in \mathbb{R}^{n \times q} \quad \text{and} \quad \boldsymbol{E} = (\boldsymbol{\epsilon}_1, \ldots, \boldsymbol{\epsilon}_n)^{\mathsf{T}} \in \mathbb{R}^{n \times q}.$$

Now, we state a condition required to describe the oracle inequality in our theoretical results.

Condition $\mathcal{M}(\mathcal{J}, \delta_{\mathcal{J}})$. *We say the design matrix $\boldsymbol{\Sigma}$ satisfies Condition $\mathcal{M}(\mathcal{J}, \delta_{\mathcal{J}})$ for an index set $\mathcal{J} \subset \{1, \ldots, p\}$ and a positive number $\delta_{\mathcal{J}}$ if*

$$\mathrm{tr}(\boldsymbol{M}^{\intercal}\boldsymbol{\Sigma}\boldsymbol{M}) \geq \delta_{\mathcal{J}} \sum_{j \in \mathcal{J}} \|\boldsymbol{M}_j\|_F^2,$$

for all $\boldsymbol{M} \in \mathbb{R}^{pK \times q}$ satisfying $2\sum_{j \in \mathcal{J}} \|\boldsymbol{M}_j\|_F \geq \sum_{j \in \mathcal{J}^c} \|\boldsymbol{M}_j\|_F$, where $\boldsymbol{M}_j$ is the collection of rows related to the jth predictor in $\boldsymbol{M}$, and $\mathrm{tr}(\cdot)$ denotes the trace of a matrix.

Condition $\mathcal{M}(\mathcal{J}, \delta_{\mathcal{J}})$ is similar to the one used in Bunea et al. (2012) for reduced rank regression models. In particular, Condition $\mathcal{M}(\mathcal{J}, \delta_{\mathcal{J}})$ is motivated by the "restricted eigenvalue" (RE) condition introduced in Bickel et al. (2009) for studying the asymptotic properties of high-dimensional linear regression. This condition implies that the least eigenvalue of the relevant predictors is greater than or equal to $\delta_{\mathcal{J}}$ by letting $\boldsymbol{M}_j = \boldsymbol{0}$, for $j \in \mathcal{J}^c$. Note that the constant 2 in the inequality $2\sum_{j \in \mathcal{J}} \|\boldsymbol{M}_j\|_F \geq \sum_{j \in \mathcal{J}^c} \|\boldsymbol{M}_j\|_F$ of Condition $\mathcal{M}(\mathcal{J}, \delta_{\mathcal{J}})$ is chosen merely for neat presentation of the statements, and it can be replaced by any positive constant greater than one. Lemma S.3 of the Supplementary Material shows that when n is at least as large as the magnitude of $|\mathcal{J}|^2 q^2 K^2 + |\mathcal{J}|^2 qK \log p$, Condition $\mathcal{M}(\mathcal{J}, \delta_{\mathcal{J}})$ holds for a constant $\delta_{\mathcal{J}} > 0$ with probability tending to one, under some mild conditions of random design.

The following assumptions are needed in our analysis.

Assumption 1. The entries of the noise matrix $\boldsymbol{E}$ are i.i.d. Gaussian random variables with mean zero and variance σ^2.

Assumption 2. The columns of the true parameters $\boldsymbol{H}_{0,(2)}$ (mode-2 matricization of $\boldsymbol{H}_0$) have Euclidean norms bounded by a constant.

Assumption 3. The domain of the exposure variable t is $\mathcal{T} = [0, 1]$. The order of the B-spline satisfies $\zeta \geq \tau + 1/2$. Let $0 = \xi_1 < \xi_2 < \cdots < \xi_{K-\zeta+2} = 1$ denote the knots of the B-spline basis. Furthermore, there exists a positive constant S_1 such that

$$h_n = \max_{k=1,\ldots,K-\zeta+1} |\xi_{k+1} - \xi_k| \asymp K^{-1} \quad \text{and} \quad h_n \Big/ \min_{k=1,\ldots,K-\zeta+1} |\xi_{k+1} - \xi_k| \leq S_1.$$

Assumption 4. The true principal functions $\beta_{0,r_2} \in \mathcal{H}$, for $r_2 = 1, \ldots, R_2$. Here, $\mathcal{H}$ is the space of functions from $[0, 1]$ to $\mathbb{R}$ satisfying the Hölder condition of order ω, that is,

$$\mathcal{H} = \big\{ g : \exists\, C \in (0, \infty) \text{ s.t. } |g^{(\iota)}(x_1) - g^{(\iota)}(x_2)| \leq C|x_1 - x_2|^\omega, \ \forall\, x_1, x_2 \in [0, 1] \big\},$$

where ι is a nonnegative integer and $g^{(\iota)}$ is the ιth derivative of g, such that $\omega \in (0, 1]$ and $\tau = \iota + \omega > 1/2$.

Assumptions 1–4 are common in the literature on nonparametric regressions (Huang et al., 2010; He et al., 2018). Specifically, Assumption 1 controls the stochastic error. Under Assumptions 3 and 4, it follows from Lemma 5 of Stone (1985) that there exists $\boldsymbol{B}_{0,r_2} = (B_{0,r_2,1}, \ldots, B_{0,r_2,K})^\mathsf{T}$ such that, for some constant S_2,

$$\left\| \beta_{0,r_2} - \sum_{k=1}^{K} B_{0,r_2,k} b_k \right\|_\infty \leq \frac{S_2}{K^\tau}, \quad r_2 = 1, \ldots, R_2, \tag{5.1}$$

where $\| \cdot \|_\infty$ is the uniform norm of functions. Let $\boldsymbol{B}_0 = (\boldsymbol{B}_{0,1}, \ldots, \boldsymbol{B}_{0,R_2})^\mathsf{T} \in \mathbb{R}^{K \times R_2}$ and

$$\boldsymbol{G}_0 = \boldsymbol{S}_0 \times_1 \boldsymbol{A}_0 \times_2 \boldsymbol{B}_0 \times_3 \boldsymbol{C}_0 \in \mathbb{R}^{p \times K \times q}.$$

Note that $\{\boldsymbol{G}_0 \,\bar{\times}_2\, \boldsymbol{b}(t)\}^\mathsf{T} \boldsymbol{x}$ is only an approximation of the true regression function, owing to the nonparametric nature of the MVCM. Using the matricization operator of a tensor (Kolda and Bader, 2009), it can be shown that

$$\{\boldsymbol{G}_0 \,\bar{\times}_2\, \boldsymbol{b}(t_i)\}^\mathsf{T} \boldsymbol{x}_i = \boldsymbol{G}_{0,(3)} \boldsymbol{z}_i, \quad i = 1, \ldots, n, \tag{5.2}$$

where $\boldsymbol{G}_{0,(3)}$ is the mode-3 matricization of $\boldsymbol{G}_0$. By (5.1), (5.2), and Assumption 2, the approximation error over n observations, $\boldsymbol{R} := \boldsymbol{Y} - \boldsymbol{E} - \boldsymbol{Z}\boldsymbol{G}_{0,(3)}^{\mathsf{T}}$, satisfies

$$\|\boldsymbol{R}\|_F^2 = \|\boldsymbol{Y} - \boldsymbol{E} - \boldsymbol{Z}\boldsymbol{G}_{0,(3)}^{\mathsf{T}}\|_F^2 \leq S_3 \frac{nsq}{K^{2\tau}}, \tag{5.3}$$

for some positive constant S_3, where s is the number of relevant predictors.

In addition, for any $\boldsymbol{G} \in \mathbb{R}^{p \times K \times q}$ with rank restrictions $\text{rank}_d(\boldsymbol{G}) \leq R_d$, for $d = 1, 2, 3$, we write

$$\Delta_{\boldsymbol{G}} = \left\{ \sum_{i=1}^n \|\{\boldsymbol{G} \,\bar{\times}_2\, \boldsymbol{b}(t_i)\}^{\mathsf{T}} \boldsymbol{x}_i - \{\boldsymbol{G}_0 \,\bar{\times}_2\, \boldsymbol{b}(t_i)\}^{\mathsf{T}} \boldsymbol{x}_i\|^2 \right\}^{1/2} \tag{5.4}$$

as the discrepancy between $\boldsymbol{G}$ and $\boldsymbol{G}_0$ in terms of prediction. Similarly, we write

$$\Delta_{\boldsymbol{F}} = \left\{ \sum_{i=1}^n \|\boldsymbol{F}(t_i)^{\mathsf{T}} \boldsymbol{x}_i - \boldsymbol{F}_0(t_i)^{\mathsf{T}} \boldsymbol{x}_i\|^2 \right\}^{1/2} \tag{5.5}$$

as the discrepancy between the coefficient functions $\boldsymbol{F}(\cdot)$, with $\boldsymbol{F}(\cdot) = \boldsymbol{G} \,\bar{\times}_2\, \boldsymbol{b}(\cdot)$ and $\boldsymbol{F}_0(\cdot)$. The following Theorem 1 shows the prediction accuracy for a solution $\widehat{\boldsymbol{G}}$ of (3.5); and its proof is deferred to Section S.2 of the Supplementary Material.

Theorem 1. *Let $\mathcal{J}(\boldsymbol{G})$ be the index set of nonzero rows of $\boldsymbol{G}_{(1)}$, the mode-1 matricization of $\boldsymbol{G}$ with $\text{rank}_d(\boldsymbol{G}) \leq R_d$, for $d = 1, 2, 3$, and denote $R = \min(R_1 R_2, R_3)$. Suppose Assumptions 1–4 hold. Taking*

$$\lambda^2 = S_4 R_3 R n \lambda_{\max}(\boldsymbol{\Sigma}) K \sigma^2 \{1 + \log(p)\}, \tag{5.6}$$

for some constant $S_4 > 0$, we then have

$$\Delta_{\widehat{\boldsymbol{G}}}^2 \leq S_5 \Delta_{\boldsymbol{G}}^2 + S_6 q R \sigma^2 + S_7 \frac{R_3 R K |\mathcal{J}(\boldsymbol{G})| \lambda_{\max}(\boldsymbol{\Sigma}) \sigma^2 \log(p)}{\delta_{\mathcal{J}(\boldsymbol{G})}} + S_8 \frac{nsq}{K^{2\tau}}, \tag{5.7}$$

with probability at least

$$1 - \frac{8 \exp(-q/2)}{3K \log(p)}, \tag{5.8}$$

provided $\boldsymbol{\Sigma}$ *satisfies Condition* $\mathcal{M}(\mathcal{J}(\boldsymbol{G}), \delta_{\mathcal{J}(\boldsymbol{G})})$, *where* $S_5, \ldots, S_8$ *are positive constants.*

Theorem 1 shows the finite-sample oracle inequality for the prediction error between the proposed estimator and its oracle spline approximation. Because the proposed Algorithm 1 may not guarantee that the generated sequence converges to a global minimum of the optimization problem, we remark that there is a gap between the oracle inequality for the global optimizer and the practical output from the proposed block updating algorithm.

For the coefficient functions, we correspondingly denote $\widehat{\boldsymbol{F}}(t) = \widehat{\boldsymbol{G}} \, \bar{\times}_2 \, \boldsymbol{b}(t)$, where $\widehat{\boldsymbol{G}}$ is a solution to (3.5). Theorem 1 can then be generalized to the prediction error for $\widehat{\boldsymbol{F}}(t)$ in terms of (5.5), as shown in the following corollary. The proof of Corollary 1 is deferred to Section S.3 of the Supplementary Material.

Corollary 1. *We have*

$$\Delta^2_{\widehat{\boldsymbol{F}}} \leq 2S_5 \Delta^2_{\boldsymbol{G}} + 2S_6 qR\sigma^2 + 2S_7 \frac{R_3 RK |\mathcal{J}(\boldsymbol{G})| \lambda_{\max}(\boldsymbol{\Sigma}) \sigma^2 \log(p)}{\delta_{\mathcal{J}(\boldsymbol{G})}} + (2S_8 + 2S_3) \frac{nsq}{K^{2\tau}}$$

with probability at least (5.8), *under the same conditions as those of Theorem 1.*

One direct application of Theorem 1 is to obtain the rate of convergence for the prediction accuracy of the proposed estimator. We can also show that the relevant predictors can be identified, with probability tending to one. In the following, let $\|f_{0,jl}\|_2$ be the L_2-norm of $f_{0,jl}$ under the Lebesgue measure, and $\widehat{f}_{jl}$ be the estimated coefficient function of $f_{0,jl}$ from (3.7). The proof of Corollary 2 is deferred to Section S.3 of the Supplementary Material.

Corollary 2. *Suppose Assumptions 1–4 hold and* $\boldsymbol{\Sigma}$ *satisfies Condition* $\mathcal{M}(\mathcal{J}(\boldsymbol{G}_0), \delta_{\mathcal{J}(\boldsymbol{G}_0)})$. *If we let*

$$K \asymp \left\{ \frac{n \delta_{\mathcal{J}(\boldsymbol{G}_0)} q}{R_3 R \lambda_{\max}(\boldsymbol{\Sigma}) \log(p)} \right\}^{1/(2\tau+1)},$$

and λ^2 is given as in (5.6), then the prediction error $\Delta^2_{\widehat{\boldsymbol{F}}}/n$ of the estimated coefficient functions
$\widehat{\boldsymbol{F}}$ *satisfies*

$$\Delta^2_{\widehat{\boldsymbol{F}}}/n = O_p\left(\frac{qR}{n} + \left\{\frac{R_3 R \lambda_{\max}(\boldsymbol{\Sigma})\log(p)}{n\delta_{\mathcal{J}(\boldsymbol{G}_0)}}\right\}^{2\tau/(2\tau+1)} sq^{1/(2\tau+1)}\right). \tag{5.9}$$

Furthermore, if

$$\frac{q^{(4\tau+1)/(2\tau+2)}\delta_{\mathcal{J}(\boldsymbol{G}_0)}^{-1/(2\tau+2)}R\{R_3\lambda_{\max}(\boldsymbol{\Sigma})\log(p)\}^{-\tau/(\tau+1)}}{n}$$
$$+ \frac{s^{(2\tau+1)/\tau}q^{1/(2\tau)}\delta_{\mathcal{J}(\boldsymbol{G}_0)}^{-(4\tau+1)/(2\tau)}R_3 R \lambda_{\max}(\boldsymbol{\Sigma})\log(p)}{n} \to 0 \tag{5.10}$$

as $n \to \infty$ and $\sum_{l=1}^{q}\|f_{0,jl}\|_2^2 \geq S_9$, for some constant $S_9 > 0$, $\forall j \in \mathcal{J}(\boldsymbol{G}_0)$, we then have

$$\mathbb{P}\{\widehat{\boldsymbol{F}}_j(t) \neq \boldsymbol{0},\ j \in \mathcal{J}(\boldsymbol{G}_0)\} \to 1 \ as \ n \to \infty,$$

where $\widehat{\boldsymbol{F}}_j^{\mathsf{T}}(t) = (\widehat{f}_{j1}, \ldots, \widehat{f}_{jq})$ is the jth row $\widehat{\boldsymbol{F}}$.

As discussed in Section 2, Models (2.3) (Lian and Ma, 2013) and (2.4) (He et al., 2018) can be regarded as special cases of our proposed all-mode reduction method. The derived rate of convergence in (5.9) includes those of He et al. (2018) and Lian and Ma (2013) as special cases, with an extra $\log p$ term due to the use of a different penalization method. Condition (5.10) for the variable selection consistency indicates that the sample size n should be sufficiently large relative to the numbers of relevant predictors s and responses q. A simple and sufficient condition for (5.10) to hold is that n should be larger than the magnitude of $q^2 s^4 R_3 R \lambda_{\max}(\boldsymbol{\Sigma})\log(p)\delta_{\mathcal{J}(\boldsymbol{G}_0)}^{-2}$.

6.   Experiments

6.1   Synthetic Data

We conduct a simulation study to evaluate the performance of the proposed model. The data are simulated from the following model:

$$y_{il} = \sum_{j=1}^{p} f_{jl}(t_i)x_{il} + \varepsilon_{il}, \quad i = 1, \ldots, n; \, l = 1, \ldots, q,$$

where $\{\varepsilon_{il}\}$ are i.i.d. random variables with normal distribution $\mathcal{N}(0, \sigma^2)$. We set $x_{i1} = 1$ as the intercept for all i, and the remaining $p-1$ predictors are generated from a multivariate Gaussian distribution with mean zero and covariance $\mathrm{Cov}(x_{ij_1}, x_{ij_2}) = \rho^{|j_1 - j_2|}$, $1 \leqslant j_1, j_2 \leqslant p-1$. The exposure variable t_i is generated from the uniform distribution on $[0, 1]$, for $i = 1, \ldots, n$, and $\{f_{jl}\}$ are generated according to the all-mode reduction model, as in (2.7). In particular, the elements of $\boldsymbol{S} \in \mathbb{R}^{R_1 \times R_2 \times R_3}$ and $\boldsymbol{C} \in \mathbb{R}^{q \times R_3}$ are i.i.d. $\mathcal{N}(0, 1)$ random variables. We let the first s predictors, including the intercept, be the truly relevant predictor variables, and the remaining $p - s$ predictors have no effect on the responses $\{y_{il}\}$. Therefore, we generated the entries of the first s rows of $\boldsymbol{A} \in \mathbb{R}^{p \times R_1}$ independently from $\mathcal{N}(0, 1)$, and the remaining rows are set as zero.

We set $R_1 = R_2 = R_3 = 2$, $p = 51$ or 201, $s = 11$, $q = 15$, and $\rho = 0.3$. We choose σ^2 according to the signal-to-noise ratio (SNR), $\mathrm{trace}\{\mathrm{Var}(\sum_{j=1}^{p} f_{jl}(t_i)x_{il})\}/q\sigma^2$. More specifically, we investigate two SNRs, 20 and 2, in our simulation study. The normalized principal functions are specified as $\boldsymbol{\beta}(t) = (\beta_1(t), \beta_2(t))^{\mathsf{T}} = (\sqrt{2}\cos(\pi t), \sqrt{2}\sin(2\pi t))^{\mathsf{T}}$ on the domain $t \in [0, 1]$, which satisfy $\int \boldsymbol{\beta}(t)\boldsymbol{\beta}(t)^{\mathsf{T}}\,\mathrm{d}t = \boldsymbol{I}_2$, a 2×2 identity matrix. We consider two sample sizes, 200 and 400. For each scenario, we generate 50 replicates of data sets.

To fit our model on each simulated data set, all the tuning parameters of the proposed

method are selected as discussed in Section 4.6. We refer to our proposed method as the all-mode reduction in the following discussion.

We compare the all-mode reduction with four alternative methods: the mode-3 reduction model (Lian and Ma, 2013), the mode-2 reduction model (He et al., 2018), the full model, and the linear model. Here, the full model refers to (2.2) with the group lasso method (Yuan and Lin, 2006) employed to select the relevant predictors. We can set $R_1 = p$, $R_2 = K$, and $R_3 = q$ in our model and use Algorithm S.1 of the Supplementary Material to solve the estimator of the full model. In the linear model, the regression coefficients are assumed to be constants, and the group lasso method is also employed. Both the full model and the linear model have the tuning parameter λ. To select λ, we use the same hold-out method as in our model for the full model, and cross-validation for the linear model. The mode-3 reduction model corresponds to dimension reduction in the responses. Therefore, its estimator can be obtained by setting $R_1 = p$ and $R_2 = K$ in our model and iteratively updating $\boldsymbol{S}$ and $\boldsymbol{C}$ using Algorithm S.1 of the Supplementary Material and (4.9). The tuning parameters R_3 and λ are selected using the hold-out method. As for the mode-2 reduction model, we apply the implementation provided in He et al. (2018), who use cross-validation to select the tuning parameters R_2 and λ.

In terms of variable selection, we calculate "True Discovery" as the average number of predictors selected by various methods that are actually relevant, and used "False Discovery" to stand for the average number of predictors selected by various methods that are actually irrelevant. The variable selection performance of the competing methods is summarized in Tables 1 and 2 for sample sizes $n = 200$ and $n = 400$, respectively, together with the performance of the rank selection $\widehat{R}_1$, $\widehat{R}_2$, and $\widehat{R}_3$ for the corresponding methods. Note that the reported selected ranks

are the average values of 50 replicates. Tables 1 and 2 show that the proposed all-mode reduction model identifies all nonzero varying-coefficient functions with the fewest number of false discovery among the competing methods. Though the full and linear models have high accuracy in terms of identifying the relevant predictors, their poor performance in terms of false discovery show that they falsely include many irrelevant predictors in their estimators. The mode-2 and mode-3 reduction methods have similar performance, and do not always correctly identify the true nonzero varying coefficients, especially when the SNR is relatively small. For the rank selections, it is shown that the third rank can be correctly selected as $\widehat{R}_3 = 2$ by using our proposed model. For the first and second ranks, we find that the proposed all-mode reduction method selects more than 76% and 80% of the 50 replicates as the true rank 2, respectively, in the setting of $p = 51$, $n = 200$, and the SNR is 20. On average, the proposed all-mode method may tend to select $\widehat{R}_1$ and $\widehat{R}_2$ slightly larger than their true values.

To evaluate the estimation accuracy, we calculate the average integrated squared error (AISE) as

$$\text{AISE} = \frac{1}{q} \sum_{j=1}^{p} \sum_{l=1}^{q} \int_0^1 \{\widehat{f}_{jl}(t) - f_{jl}(t)\}^2 \, dt,$$

where $\widehat{f}_{jl}(t)$ denotes a generic estimator of $f_{jl}(t)$ using the various methods. The above integrals are computed using the Monte Carlo method. Table 3 reports the AISEs of the competing methods, with the corresponding standard errors. For benchmark, we add the oracle estimator which includes only the true relevant predictors in its model. In other words, the true relevant predictors are assumed to be known in the oracle setting. Therefore, we do not include the penalization in the objective function, enabling us to use the least squares method to estimate $\boldsymbol{S}$ and $\boldsymbol{A}$. We use the same framework of block updating Algorithm 1 to compute the oracle

		$\widehat{R}_1$	$\widehat{R}_2$	$\widehat{R}_3$	True Discovery	False Discovery
$p = 51$	**SNR=20**					
	All-mode Reduction	2.34	2.14	2.00	11.00 (0.00)	3.26 (0.28)
	Mode-3 Reduction	-	-	2.00	10.86 (0.55)	10.45 (0.83)
	Mode-2 Reduction	-	2.19	-	11.00 (0.00)	11.39 (0.70)
	Full Model	-	-	-	11.00 (0.00)	13.48 (0.93)
	Linear Model	-	-	-	11.00 (0.00)	19.07 (1.19)
	SNR=2					
	All-mode Reduction	2.64	2.34	2.00	11.00 (0.00)	3.65 (0.34)
	Mode-3 Reduction	-	-	2.00	10.34 (0.95)	14.43 (1.14)
	Mode-2 Reduction	-	2.25	-	11.00 (0.00)	18.75 (1.40)
	Full Model	-	-	-	11.00 (0.00)	21.31 (1.54)
	Linear Model	-	-	-	11.00 (0.00)	24.87 (1.60)
$p = 201$	**SNR=20**					
	All-mode Reduction	2.67	2.58	2.00	11.00 (0.00)	12.08 (0.59)
	Mode-3 Reduction	-	-	2.00	10.96 (0.54)	19.40 (1.15)
	Mode-2 Reduction	-	2.41	-	11.00 (0.00)	25.86 (1.46)
	Full Model	-	-	-	11.00 (0.00)	28.47 (1.96)
	Linear Model	-	-	-	11.00 (0.00)	31.51 (2.57)
	SNR=2					
	All-mode Reduction	2.57	2.60	2.00	10.44 (0.39)	15.42 (1.32)
	Mode-3 Reduction	-	-	2.00	9.96 (1.21)	19.87 (1.47)
	Mode-2 Reduction	-	2.84	-	9.83 (0.81)	23.17 (1.74)
	Full Model	-	-	-	11.00 (0.00)	36.48 (2.18)
	Linear Model	-	-	-	11.00 (0.00)	44.87 (2.45)

Table 1: Dimension reduction and variable selection results for group lasso penalized estimators

for $n = 200$. The numbers in parentheses are the standard errors based on 50 replicates.

		$\widehat{R}_1$	$\widehat{R}_2$	$\widehat{R}_3$	True Discovery	False Discovery
	All-mode Reduction	2.31	2.15	2.00	11.00 (0.00)	2.42 (0.28)
	Mode-3 Reduction	-	-	2.00	11.00 (0.00)	8.64 (0.61)
SNR=20	Mode-2 Reduction	-	2.20	-	11.00 (0.00)	8.78 (0.66)
	Full Model	-	-	-	11.00 (0.00)	11.52 (0.84)
	Linear Model	-	-	-	11.00 (0.00)	17.87 (1.15)
$p = 51$	All-mode Reduction	2.39	2.21	2.00	11.00 (0.00)	3.71 (0.34)
	Mode-3 Reduction	-	-	2.00	10.52 (0.78)	10.72 (0.90)
SNR=2	Mode-2 Reduction	-	2.23	-	11.00 (0.00)	12.38 (0.92)
	Full Model	-	-	-	11.00 (0.00)	16.86 (1.01)
	Linear Model	-	-	-	11.00 (0.00)	21.87 (1.45)
	All-mode Reduction	2.45	2.50	2.00	11.00 (0.00)	10.71 (0.58)
	Mode-3 Reduction	-	-	2.00	11.00 (0.00)	18.85 (1.02)
SNR=20	Mode-2 Reduction	-	2.38	-	11.00 (0.00)	20.32 (1.38)
	Full Model	-	-	-	11.00 (0.00)	23.10 (1.82)
	Linear Model	-	-	-	11.00 (0.00)	30.51 (2.47)
$p = 201$	All-mode Reduction	2.45	2.70	2.00	10.50 (0.24)	11.83 (1.00)
	Mode-3 Reduction	-	-	2.00	10.12 (1.11)	17.57 (1.16)
SNR=2	Mode-2 Reduction	-	2.49	-	10.33 (0.93)	19.48 (1.36)
	Full Model	-	-	-	11.00 (0.00)	31.59 (2.28)
	Linear Model	-	-	-	11.00 (0.00)	43.07 (1.82)

Table 2: Similar to Table 1, but for $n = 400$.

estimator. A box plot of the AISEs for the various methods with sample size $n = 400$ is depicted in

Figure 4. We conclude from Table 3 and Figure 4 that the all-mode reduction model outperforms

other non-oracle estimators, with the smallest AISE. For example, when the sample size $n =$ 400, the all-mode reduction method reduces the AISE by 48%–94% compared with the mode-3 reduction, and by 78%–98% compared with the mode-2 reduction. The performance of the all-mode reduction method improves when the sample size increases, which is consistent with our theoretical investigation. Among the alternative methods, the full model and the linear model show the worst performance.
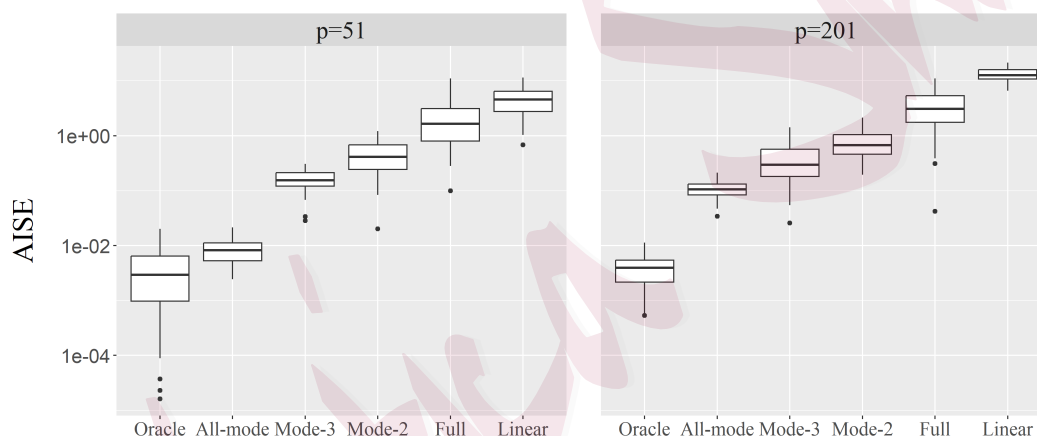

Figure 4: A box plot of the AISEs for the competing methods when $n = 400$ and the SNR is 20. The left and right panels represent the AISEs for $p = 51$ and for $p = 201$, respectively. The y-axis is measured in logarithmic scale.

6.2   Real Data

We further illustrate the proposed method on the data set from the Framingham Heart Study (FHS; Dawber et al. 1951), which aims to identify common factors that lead to cardiovascular diseases. The data set collects the measurements on 15 phenotypes from 325 patients, in addition to the single nucleotide polymorohism (SNP) information. All variables are standardized with

n	p	SNR	Oracle	All-mode Reduction	Mode-3 Reduction	Mode-2 Reduction	Full Model	Linear Model
200	51	20	0.007	0.011	0.237	0.782	3.459	6.761
			(0.002)	(0.003)	(0.019)	(0.082)	(0.339)	(0.674)
		2	0.031	0.085	0.314	1.484	6.348	10.197
			(0.004)	(0.007)	(0.015)	(0.104)	(0.454)	(0.568)
	201	20	0.008	0.223	0.496	0.794	4.327	15.192
			(0.004)	(0.051)	(0.052)	(0.084)	(0.453)	(0.961)
		2	0.042	0.293	0.615	2.940	10.361	20.387
			(0.006)	(0.009)	(0.063)	(0.281)	(0.972)	(1.623)
400	51	20	0.004	0.010	0.164	0.501	2.240	4.933
			(0.001)	(0.002)	(0.011)	(0.042)	(0.268)	(0.469)
		2	0.018	0.022	0.281	0.841	4.418	8.910
			(0.002)	(0.002)	(0.016)	(0.065)	(0.399)	(0.457)
	201	20	0.005	0.101	0.403	0.679	4.229	14.584
			(0.001)	(0.007)	(0.042)	(0.049)	(0.532)	(0.567)
		2	0.022	0.286	0.549	1.306	9.061	17.178
			(0.002)	(0.009)	(0.065)	(0.118)	(0.895)	(1.340)

Table 3: The AISEs for the competing methods. The numbers in parentheses are the standard errors based on 50 replicates.

mean zero and variance one. After matching the SNP data with the phenotypes and deleting observations with missing values and outliers, we focus on a subset of 258 patients in our analysis. We preselected six phenotypes of interest: *height, bi-deltoid girth, right arm girth-upper third,*

waist girth, *hip girth*, and *thigh girth*. The exposure variable is set as *weight*. We follow the screening procedure in Fan et al. (2014) to select 200 SNPs as predictors (the intercept is also included in the model). To fit our proposed method, all the tuning parameters are selected as discussed in Section 4.6. Specifically, we split the data set randomly into three subsets, namely, a training set, a validation set, and a test set, of size 150, 50, and 58, respectively. The training and validation sets are used to determine (R_1, R_2) and λ, and the test set is used to evaluate the out-of-sample prediction performance. The recommended rule $K = [2n^{1/5}]$ for the number of basis functions leads to $K = 6$. To evaluate the performance, the corresponding prediction error is defined as

$$\text{Prediction Error} = \frac{1}{n_{\text{test}}} \sum_{i=1}^{n_{\text{test}}} \|\boldsymbol{y}_i - \widehat{\boldsymbol{y}}_i\|_2^2,$$

where $\{\boldsymbol{y}_i\}$ are the observed responses in the test set, $\widehat{\boldsymbol{y}}_i = \{\widehat{\boldsymbol{G}} \, \bar{\times}_2 \, \boldsymbol{b}(t)\}^{\intercal} \boldsymbol{x}_i$ with the corresponding predictors $\boldsymbol{x}_i$, and n_{test} is the size of the test set. We compare the proposed model, namely the all-mode reduction, with four non-oracle alternatives in Section 6.1. Furthermore, we implement the elementwise-sparsity method on the full model to fit this data set. Here, we can achieve the full model with the elementwise-sparsity method by using the group lasso penalization (Yuan and Lin, 2006) on each coefficient function in (2.2) to select the relevant predictors for the response variables. The performance of each method is evaluated based on 50 random splittings of training, validation, and test sets.

Table 4 records the average prediction error of the competing methods on the test data and the performance of the dimension reduction. We observe in Table 4 that the full model with the row-sparsity method outperforms the elementwise-sparsity method, implying that the FHS data set may be better fitted using the row-sparsity methods than the elementwise-sparsity methods.

In addition, the proposed all-mode reduction model has the highest prediction accuracy, and achieves significant dimensionality reduction on each mode. This result is consistent with that based on the synthetic data. To investigate a biological interpretation of the identified SNPs, we input the submitted $ss\sharp$ of the identified SNPs to the NCBI database (Sherry et al., 2001) to retrieve the reference $rs\sharp$ records. The proposed all-mode reduction method identified 30 SNPs by combining the variable selection results of 50 random splits. Some of these SNPs have been confirmed scientifically. For example, the reference SNP $rs4896044$ is found to be associated with hypertension (Consortium, 2007), and $rs9321440$ has links with multiple heart diseases (Gagliardi, 2011). The mode-3 reduction method identified 51 SNPs, including all 30 SNPs selected by the all-mode reduction method. On the other hand, the mode-2 reduction method identified 47 SNPs, with 25 of the SNPs selected by the all-mode reduction method, including the scientifically confirmed $rs4896044$ and $rs9321440$.

	Prediction error	$\widehat{R}_1$	$\widehat{R}_2$	$\widehat{R}_3$
All-mode Reduction	0.4542 (0.0071)	2.7	3.1	2.0
Mode-3 Reduction	0.6011 (0.0196)	-	-	2.0
Mode-2 Reduction	0.6385 (0.0357)	-	4.3	-
Full Model (row-sparsity)	1.0181 (0.0417)	-	-	-
Full Model (elementwise-sparsity)	1.2106 (0.0403)	-	-	-
Linear Model	1.2578 (0.0488)	-	-	-

Table 4: Prediction error of the test data. The numbers in parentheses are the standard errors based on 50 replicates of random splitting.

6.3   Additional Numerical Results

To further demonstrate the utility of the proposed all-mode reduction method, we conduct additional numerical experiments, and present the results in Section S.5 of the Supplementary Material. More precisely, we extend our simulation settings to larger numbers of response variables q, and plot the trend of the performance of the proposed method when q increases in Section S.5.1 of the Supplementary Material. In Section S.5.2 of the Supplementary Material, we depict the fitted coefficient functions of the biologically confirmed SNP rs9321440 based on 50 replicates of random splitting. Our results show that rs9321440 may have different effects on the phenotypes of *height*, *bi-deltoid girth*, *right arm girth-upper third*, *hip girth*, and *thigh girth*, given distinct body weights. For the phenotype of *waist girth*, the effect of this SNP may not vary significantly with body weight. We refer readers to Section S.5 of the Supplementary Material for details.

7.   Discussion

We have proposed a dimension-reduction method based on the Tucker decomposition of a third-order tensor to estimate the varying coefficients of an MVCM under a high-dimensional setting. The proposed model unifies dimensionality reductions in three aspects: relevant predictors, coefficient functions, and responses. To take sparsity into account, we integrate a sparsity-inducing penalization into the estimation. The oracle inequality for the prediction risk of the proposed estimator is derived under fixed and random designs. We have used both simulated and real data sets to evaluate and compare the empirical performance of the proposed model with that of other methods, and the results illustrate the superior performance of our method.

One difficulty of applying the proposed method is the need to tune the ranks of the Tucker

decomposition, which may become computationally expensive when the dimension is extremely high. Developing an efficient way to tune the ranks requires further investigation. Furthermore, in some applications, the relationships between responses can be determined using external covariates, such as spatial locations, providing extra information for measuring the similarity between responses, thus inducing a (weighted) graphical structure among the tasks. Therefore, future research should extend the proposed model to the problem of graph regularized multi-task learning. Finally, incorporating the elementwise-sparsity method with the all-mode reduction model may be useful in other real applications. This, too, is left as a future research topic.

Supplementary Material

The online Supplementary Material contains: (i) the details of updating S, A, and B; (ii) the technical proofs of Theorem 1 and Corollaries 1–2; (iii) the theoretical results for the random-design settings and the corresponding proofs; and (iv) additional numerical results for the simulation study and the analysis of real data set.

Acknowledgments

References

Absil, P.-A., R. Mahony, and R. Sepulchre (2009). *Optimization algorithms on matrix manifolds.* Princeton, New Jersey: Princeton University Press.

Ahmed, T., H. Raja, and W. U. Bajwa (2020). Tensor regression using low-rank and sparse tucker decompositions. *SIAM Journal on Mathematics of Data Science 2*(4), 944–966.

Bickel, P., Y. Ritov, and A. Tsybakov (2009). Simultaneous analysis of lasso and dantzig selector. *The Annals of Statistics 37*(4), 1705–1732.

Boyd, S., N. Parikh, E. Chu, B. Peleato, and J. Eckstein (2011). Distributed optimization and statistical learning via the alternating direction method of multipliers. *Foundations and Trends® in Machine Learning 3*(1), 1–122.

Bunea, F., Y. She, and M. H. Wegkamp (2012). Joint variable and rank selection for parsimonious estimation of high-dimensional matrices. *The Annals of Statistics 40*(5), 2359–2388.

Consortium, T. W. T. C. C. (2007). Genome-wide association study of 14,000 cases of seven common diseases and 3,000 shared controls. *Nature 447*(7145), 661–678.

Dawber, T. R., G. F. Meadors, and F. E. Moore Jr (1951). Epidemiological approaches to heart disease: The framingham study. *American Journal of Public Health and the Nations Health 41*(3), 279–286.

Edelman, A., T. A. Arias, and S. T. Smith (1998). The geometry of algorithms with orthogonality constraints. *SIAM journal on Matrix Analysis and Applications 20*(2), 303–353.

Fan, J., Y. Ma, and W. Dai (2014). Nonparametric independence screening in sparse ultra-high-dimensional varying coefficient models. *Journal of the American Statistical Association 109*(507), 1270–1284.

Gabay, D. and B. Mercier (1976). A dual algorithm for the solution of nonlinear variational problems via finite element approximation. *Computers & Mathematics with Applications 2*(1), 17–40.

Gagliardi, L. (2011). *Regulation of cortisol secretion in humans: Relation to vasopressin action at the adrenals in macron-odular and micronodular adrenocortical tumours; and well-being in Addison's Disease.* Ph. D. thesis.

Gower, J. C. and G. B. Dijksterhuis (2004). *Procrustes problems.* Oxford, UK: Oxford University Press.

Hannun, A. Y., P. Rajpurkar, M. Haghpanahi, G. H. Tison, C. Bourn, M. P. Turakhia, and A. Y. Ng (2019). Cardiologist-level arrhythmia detection and classification in ambulatory electrocardiograms using a deep neural network. *Nature Medicine 25*(1), 65–69.

Harshman, R. (1970). Foundations of the parafac procedure: Models and conditions for an "explanatory" multi-mode factor analysis. *UCLA Working Papers in Phonetics 16*, 1–84.

Hastie, T. and R. Tibshirani (1993). Varying-coefficient models. *Journal of the Royal Statistical Society: Series B (Method-ological) 55*(4), 757–779.

He, K., H. Lian, S. Ma, and J. Z. Huang (2018). Dimensionality reduction and variable selection in multivariate varying-coefficient models with a large number of covariates. *Journal of the American Statistical Association 113*(522), 746–754.

He, L., F. Wang, K. Chen, W. Xu, and J. Zhou (2018). Boosted sparse and low-rank tensor regression. In *Advances in Neural Information Processing Systems*, Volume 31, pp. 1009–1018.

Hoover, D. R., J. A. Rice, C. O. Wu, and L.-P. Yang (1998). Nonparametric smoothing estimates of time-varying coefficient models with longitudinal data. *Biometrika 85*(4), 809–822.

Huang, J., J. L. Horowitz, and F. Wei (2010). Variable selection in nonparametric additive models. *The Annals of Statistics 38*(4), 2282.

Huang, J. Z., C. O. Wu, and L. Zhou (2002). Varying-coefficient models and basis function approximations for the analysis of repeated measurements. *Biometrika 89*(1), 111–128.

Huang, J. Z., C. O. Wu, and L. Zhou (2004). Polynomial spline estimation and inference for varying coefficient models

    with longitudinal data. *Statistica Sinica 14*(3), 763–788.

Hunter, D. R. and K. Lange (2004). A tutorial on mm algorithms. *The American Statistician 58*(1), 30–37.

Hunter, D. R. and R. Li (2005). Variable selection using mm algorithms. *The Annals of Statistics 33*(4), 1617–1642.

Jiang, Q., H. Wang, Y. Xia, and G. Jiang (2013). On a principal varying coefficient model. *Journal of the American

    Statistical Association 108*(501), 228–236.

Kolda, T. G. and B. W. Bader (2009). Tensor decompositions and applications. *SIAM Review 51*(3), 455–500.

Li, X., D. Xu, H. Zhou, and L. Li (2018). Tucker tensor regression and neuroimaging analysis. *Statistics in Biosciences 10*(3),

    520–545.

Lian, H. (2012). Variable selection for high-dimensional generalized varying-coefficient models. *Statistica Sinica 22*(4),

    1563–1588.

Lian, H. and S. Ma (2013). Reduced-rank regression in sparse multivariate varying-coefficient models with high-dimensional

    covariates. *arXiv preprint arXiv:1309.6058*.

Liu, J., R. Li, and R. Wu (2014). Feature selection for varying coefficient models with ultrahigh-dimensional covariates.

    Journal of the American Statistical Association 109(505), 266–274.

Lu, W., Z. Zhu, and H. Lian (2020). High-dimensional quantile tensor regression. *Journal of Machine Learning Re-

    search 21*(250), 1–31.

Oseledets, I. V. (2011). Tensor-train decomposition. *SIAM Journal on Scientific Computing 33*(5), 2295–2317.

Park, B. U., E. Mammen, Y. K. Lee, and E. R. Lee (2015). Varying coefficient regression models: A review and new

    developments. *International Statistical Review 83*(1), 36–64.

Ruppert, D., M. P. Wand, and R. J. Carroll (2003). *Semiparametric regression*. Cambridge: Cambridge University Press.

Sherry, S. T., M.-H. Ward, M. Kholodov, J. Baker, L. Phan, E. M. Smigielski, and K. Sirotkin (2001). Dbsnp: The ncbi database of genetic variation. *Nucleic Acids Research 29*(1), 308–311.

Stone, C. J. (1985). Additive regression and other nonparametric models. *The Annals of Statistics 3*(2), 689–705.

Tucker, L. R. (1966). Some mathematical notes on three-mode factor analysis. *Psychometrika 31*(3), 279–311.

Wang, L., H. Li, and J. Z. Huang (2008). Variable selection in nonparametric varying-coefficient models for analysis of repeated measurements. *Journal of the American Statistical Association 103*(484), 1556–1569.

Wei, F., J. Huang, and H. Li (2011). Variable selection and estimation in high-dimensional varying-coefficient models. *Statistica Sinica 21*(4), 1515–1540.

Xue, L. and A. Qu (2012). Variable selection in high-dimensional varying-coefficient models with global optimality. *Journal of Machine Learning Research 13*(1), 1973–1998.

Yuan, M. and Y. Lin (2006). Model selection and estimation in regression with grouped variables. *Journal of the Royal Statistical Society: Series B (Statistical Methodology) 68*(1), 49–67.

Zhou, H., L. Li, and H. Zhu (2013). Tensor regression with applications in neuroimaging data analysis. *Journal of the American Statistical Association 108*(502), 540–552.

Fengyu Zhang and Kejun He (Email: kejunhe@ruc.edu.cn)

Center for Applied Statistics, Institute of Statistics and Big Data, Renmin University of China, Beijing 100872, China.

Ya Zhou

Department of Information Center, Fuwai Hospital, Chinese Academy of Medical Sciences and Peking Union Medical College, Beijing 100037, China.

Raymond K. W. Wong

Department of Statistics, Texas A&M University, College Station 77843, USA.